Spring 5-13-2021

Distribution of Contamination Sources in the Atlanta Metropolitan Area along the Upper Chattahoochee River Basin: An Environmental Justice Focus

Ahmadou T. Deme

DISTRIBUTION OF CONTAMINATION SOURCES IN THE ATLANTA METROPOLITAN AREA ALONG THE UPPER CHATTAHOOCHEE RIVER BASIN: AN ENVIRONMENTAL JUSTICE FOCUS

by

AHMADOU TIDIANE DEME

Under the Direction of Hassan Babaie, PhD

ABSTRACT

Over the last few decades, the rapid expansion of the Atlanta urban area has led to the increase of the number of sources of pollutions around the area and the level of pollution in the Chattahoochee River. This research analyzed the change in the distribution of sources of contamination over time and space, and evaluated their impact on environmental justice in the Atlanta metropolitan area. The results indicate contaminated areas increased from 2000 to 2019, spreading from the central metropolitan area to the south along the Chattahoochee River. The Box and whisker plots indicated existence of spatio-temporal variations in the water quality parameters, with Ca, Mg, Fe, SiO_2, NO_3, and Cl displaying a relatively large length of boxes and whiskers compared to other parameters. The results show a disproportionate exposure to environmental hazards regarding income, race, age, and sex, and no application of environmental justice principles to the study area.

INDEX WORDS: Contamination, Surface water, Environmental justice, GIS

DISTRIBUTION OF CONTAMINATION SOURCES IN THE ATLANTA METROPOLITAN AREA ALONG THE UPPER CHATTAHOOCHEE RIVER BASIN: AN ENVIRONMENTAL JUSTICE FOCUS

by

AHMADOU TIDIANE DEME

A Thesis Submitted in Partial Fulfillment of the Requirements for the Degree of

Master of Science

in the College of Arts and Sciences

Georgia State University

2021

DISTRIBUTION OF CONTAMINATION SOURCES IN THE ATLANTA METROPOLITAN AREA ALONG THE UPPER CHATTAHOOCHEE RIVER BASIN: AN ENVIRONMENTAL JUSTICE FOCUS

by

AHMADOU TIDIANE DEME

Committee Chair: Hassan Babaie

Committee: Armita Davarpanah

Dajun Dai

Na'Taki Jelks

Electronic Version Approved:

Office of Graduate Services

College of Arts and Sciences

Georgia State University

May 2021

DEDICATION

I dedicate this thesis to my deceased father, Maoloudou DEME, as proof of respect and gratitude. I would also like to dedicate this to my mother, Adji Gaye for the special role she has always played in my life. And, to all those who have directly or indirectly contributed to the achievement of this work.

ACKNOWLEDGEMENTS

First and foremost, I am extremely grateful to my thesis advisors, Dr. Babaie and Dr. Davarpanah for the continuous support, and patience during my thesis study. The development and completion of this thesis would have never been possible without their guidance and support.

I would also like to thank Dr. Dai and Dr. Jelks for serving as committee advisors, and Department of Geosciences, GSU, for the funding support.

I am also grateful to Dr. Kabengi, Graduate Director of the Department of Geosciences, for providing me with valuable guidance and encouragement during my graduate career.

TABLE OF CONTENTS

ACKNOWLEDGEMENTS ..... **V**

LIST OF TABLES ..... **IX**

LIST OF FIGURES ..... **X**

1 INTRODUCTION **1**

1.1 Background and Problem Statement **1**

1.2 Purpose of the Study **5**

1.3 Research Questions **6**

2 LITERATURE REVIEW **7**

2.1 GIS and Point and Non-Point Source Pollutions **7**

2.2 DRASTIC Model and Groundwater Contamination **10**

2.3 GIS and Environment Justice Assessment **13**

3 METHODS AND PROCEDURES **16**

3.1 General area description **16**

3.1.1 Geographical context ***16***

3.1.2 Geological and hydrogeological setting ***20***

3.1.3 Soils of the study area ***22***

3.2 Data collection **23**

3.3 Methods **25**

3.3.1 Mann–Kendall test and Sen's slope estimation method ***25***

3.3.2 Principal component analysis (PCA) *27*

3.3.3 Spatial pattern analysis of contaminant sources (K-Function) *28*

3.3.4 Lineament extraction and analysis *29*

4 RESULTS **32**

4.1 Spatio-Temporal Variations of Water Quality Parameters **32**

4.2 Trend in Surface Water Quality **40**

4.2.1 Trend over Time *40*

4.2.2 Trend over Latitude of the location of the sample sites *41*

4.3 Principal factor governing geochemical processes **42**

4.4 Lineament and density maps of the study area **46**

4.5 Land Use and Land Cover (LULC) Analysis **48**

4.6 Multi-distance spatial cluster analysis of contaminant sources **49**

4.7 Spatio-temporal variations of quantity of chemicals released in the study area .. **52**

4.8 Environmental justice analysis **57**

4.8.1 Distribution of TRI facilities and onsite release by income *57*

4.8.2 Distribution of TRI facilities and onsite release by race *60*

4.8.3 Distribution of TRI facilities and onsite release by age *65*

4.8.4 Distribution of TRI facilities and onsite release by sex *68*

5 DISCUSSIONS **71**

5.1 Spatio-Temporal Variations and Trend Analyses **71**

5.2 Geochemical Processes and Sources of Contamination..... 73

5.3 Correlation of Sources of Contamination with Lineament And LULC 74

5.4 Correlation of Sources of Contaminations with Low-Income Communities and People of Color 77

5.5 Limitations..... 78

5.6 Future Recommendations 79

REFERENCES..... 81

LIST OF TABLES

Table 4-1 Univariate analysis of surface water quality parameters in 2000, 20003, 2006, 2012, 2015, and 2019 33

Table 4-2 Mann Kendall trends and Sen's Slope Estimator of Parameters from 2000 to 2019 ... 41

Table 4-3 Nature and magnitude of trend in water quality parameters over the decreasing latitude of the station. 42

Table 4-4 Total variance explained 43

Table 4-5 Principal component loadings for varimax rotated factor matrix explaining 84.228% of the total variances 44

Table 4-6 Parameters grouping based on the nature of the principal component loadings 44

Table 4-7 Matrix of correlation coefficients for hydrochemical data in the study area 45

LIST OF FIGURES

Figure 3-1 Map of the Apalachicola-Chattahoochee River Basin (Riverkeeper 17

Figure 3-2 Chattahoochee River Basin across Atlanta metropolitan 19

Figure 3-3 Map of Georgia Primary Aquifers (USGS, 1997, modified) 21

Figure 3-4 Atlanta Underlying Bedrock Geology (USGS, 1997) 22

Figure 3-5 Surface Water Sample Sites 26

Figure 4-1 Box-whisker plots of surface water quality parameters 34

Figure 4-2 Lineament map and lineament density map (magnitude-per-unit area) of Atlanta metropolitan 47

Figure 4-3 LULC Map of Atlanta Metropolitan 48

Figure 4-4 Distribution of TRI facilities across Atlanta metropolitan from 2000 to 2019 50

Figure 4-5 K Function graphs of TRI from 2000 to 2019 in Atlanta metropolitan. 51

Figure 4-6 Toxic Release Inventory (TRI) in 2000 and 2003 53

Figure 4-7 Toxic Release Inventory (TRI) in 2006 and 2009 54

Figure 4-8 Toxic Release Inventory (TRI) in 2012 and 2015 55

Figure 4-9 Toxic Release Inventory (TRI) in 2019 56

Figure 4-10 TRI Facilities distribution and households median income in 2019 58

Figure 4-11 TRI Onsite Release and Households Median Income in 2019 59

Figure 4-12 TRI Facilities distribution and black and white population in 2019 61

Figure 4-13 TRI Facilities distribution and ratio of black over white population in 2019 62

Figure 4-14 TRI onsite release and black and white population in 2019 63

Figure 4-15 TRI onsite release and ratio of black over white population in 2019 64

Figure 4-16 TRI facilities distribution and median age in 2019 66

Figure 4-17 TRI onsite release and median age in 2019 67

Figure 4-18 TRI Facilities distribution and sex ratio (males per 100 females) in 2019 69

Figure 4-19 TRI Onsite Release and Sex Ratio (Males per 100 Females) in 2019 70

Figure 5-1 Correlations between Lineament Density Map and TRI Onsite Release in 2019..... 75

Figure 5-2 Correlations between LULC and TRI Onsite Release in 2019 76

1 INTRODUCTION

1.1 Background and Problem Statement

The current world's urban population of more than 4 billion people is projected to increase to close to 7 billions by 2050 *(UN DESA, 2014).* Urbanization is relatively a new trend in human history and directly influences the population growth rate and ecology in every nation. Most urban inhabitants rapidly increase their ecological footprint by altering their physical environment through increased consumption of food, energy, water, and land, which has led to their depletion or degradation over the last century (Satterthwaite et al., 2010). Intensive urban growth and agricultural activities lead to the degradation of the surface and groundwater quality and quantity due to the excessive withdrawals in urban, peri-urban, and rural areas (Shabnam et al., 2017; Satterthwaite et al., 2010; Cohen and Garrett 2009). Most pollutants enter water resources from industrial and commercial facilities such as hazardous waste sites (e.g., oil and chemical spills), non-point sources (e.g., roads, parking lots, and storm drain), wastewater treatment plants, and sewage systems. The key problem in the sustainable management of water resources is identifying the effective sources of water pollutions. Thus, mapping the sources of contamination has become one of the important challenging issues over the past decade (Shabnam et al., 2017).

Over the last few decades, the Metropolitan Atlanta area has been one of *the fastest*-growing cities in the U.S. (with nation's 4th highest population growth) by many measures such as rapid economic development. The population of the city of Atlanta is projected to triple by 2025. The extent of this largest metropolitan area in the southeast is also projected to increase by about 928,379 ha between 1999 and 2050, which corresponds to a rate of about 50 ha per day, and represents an increase of 254% for the entire period (Yang and Lo, 2003). This expansion of urban centers has consequently led to the increase in the number of sources of pollution from industries,

farms, chicken farms, factories, storages, gas station, sewer foul, waste sites, etc., and the amount of urban runoff carrying polluted stormwater (Rose and Peters, 2001). Typical impacts also include an increase in chemical loads to local and downstream collecting waters from industrial sources, leaking sewer systems and sewer overflows, and soil contamination from industrial sources (Rose and Peters, 2001). Numerous industries are based in Atlanta producing tremendous amounts of chemical and other toxic substances that, if not handled with care, could have a significant impact on the environment when spilled into water resources and soil (Stack & Associates, 2018). Moreover, Atlanta's water and sewer infrastructures are aged (built in the 1880s) and have experienced numerous cracks in both water and sewer lines (Clean Water Atlanta, 2010).

Due to the problems mentioned above, the level of pollution in the Chattahoochee River has been rising over the last few decades (EPA, 2018). Sewage, pollutants, trash, and bacteria from the tributaries continuously feed into the Chattahoochee River. State and federal environmental officials have found 'hundreds' of companies and have been suing the ones in the Chattahoochee watershed that violated Clean Water Laws. The river struggles with sewage spills and higher levels of bacteria and pollutants after heavy rains especially when the temperature rises in the summer (Dusen et al., 2017). With the growth of metropolitan Atlanta, severe water pollution from sewer overflows and sediment inflow have affected water quality in the Chattahoochee River (Cook, 2018). In 1995, the city of Atlanta was sued for violating the Clean Water Act (EPA, 1999), and in 2000, a federal consent decree instructed the City of Atlanta to clean up 568 tons of trash and remove seven automobiles, that fed into the Chattahoochee. Stormwater carries a large volume of trash and litter from roads, parks, etc. into the River where it can break down and become a serious issue (EPA, 1999).

To protect and restore the Chattahoochee River and monitor its water quality, several state and federal laws were signed by the Environmental Protection Division of Georgia (EPD), the City of Atlanta, and the Environmental Protection Agency (EPA). In 1973, the Metropolitan River Protection Act was enacted by the state of Georgia (Georgia General Assembly), setting strict rules on new development to establish a 2000 feet Corridor within the Chattahoochee River and impound it within 48 miles between Buford Dam and Peachtree (Dusen et al., 2017). Thus, the act forced the Atlanta Regional Commission and local governments along the corridor to adopt a plan to protect the River Corridor and monitor land-disturbing activity in the corridor. In 1998, a Federal Consent Decree was signed by Mayor Bill Campbell to improve water quality in the Chattahoochee River, Atlanta metropolitan streams, and South Rivers. The Consent Decree committed the city of Atlanta to develop an accelerated program of activities to end water quality violations resulting from sewer overflows by 2007 (Cook, 2018). The sewer improvement program would include the evaluation of sewer pipe conditions, and rehabilitation or replacement of defected or capacity limited sewer lines (EPA, 1999). In February 2017, a member of Congress instructed the U.S. EPA to evaluate Atlanta's compliance with the city's Combined Sewer Overflow Consent Decree by (EPA, 2018). As a result, according to the Office of Inspector General of the EPA (2018), Atlanta completed its combined sewer overflow improvement projects by 2008 and complied with the Consent Decree, but the city has not yet met all the requirements (EPA, 2018). The city continues to work on those projects and has to complete them by 2027, as extended by the 2012 amendment. Furthermore, several other state and federal laws and volunteers such as the Upper Chattahoochee Riverkeeper, the Safe Drinking Water Act, the State Water Quality Control Act, and the Federal Clean Water Act were instated to protect the Chattahoochee

River from pollutants, and inspect hundreds of industrial operations annually by providing guidance for compliance with applicable laws and permits (EPD, 1997).

Significant improvements in the quality of water and the effects of sources of pollution affecting the Chattahoochee River were noted after implementing the aforementioned federal and state laws. The River water quality has improved compared to what it has been over the last decade, and contamination from sewage overflows to the River has decreased with the implementation of the Consent Decree (Dusen et al., 2017). In 2012, Atlanta reported to the District Court that the volume of sewage overflows had been removed by 95 percent since 2004, and at the end of 2017, the City also reported to have completed 72 percent of its sewer system construction projects and two of its six sewersheds (EPA, 2018). However, despite the advancements and improvements that were made in the decade, the River is still exposed to a high level of bacteria and pollutants.

Regarding the impacts on environmental justice, people of color and low-income in Atlanta often suffer disproportionately from sewage overflow, toxic release, factory pollution, and other effects of toxic pollution. Georgia's Environmental Protection Division (EPD) does not have an official environmental justice policy requiring the consideration of demographics or socioeconomic factors before issuing a permit (David, 2012). In 1995, the Georgia Environmental Justice Act of 1995 was proposed in Georgia's legislature that would have required the consideration of the demographics of an area before issuing a permit. However, the bill did not pass. Two years later, the Environmental Justice Act of 1997, that would have required EPD to issue an annual state toxic release inventory report on the amount of toxic chemicals released by manufacturers, and to assess its risk to affect the public health or nearby communities' environment, was also unsuccessful. A decade later, the Georgia Brownfields Rescue, Redevelopment, Community Revitalization and Environmental Justice Act of 2006 was proposed.

The bill would have addressed the issue of an unacceptably high percentage of brownfields in minority-and-low-income communities. It also did not pass (David, 2012). Georgia's "anti-concentration" law, passed in 2004, is the only law that requires some consideration of environmental justice principles. However, it does not address the demographics of the area where facilities might locate. While EPD does not have an official environmental justice policy, the ideas are integrated into its mission, value, and guiding principles. EPD believes that all Georgians have a right to a healthy environment and equitable enforcement of environmental laws (EPA, 2018).

1.2 Purpose of the Study

Analyze the distribution of sources of contamination over time and space (spatial and temporal variations), and correlate pollution sources with the location of marginalized and low-income communities as well as people of color who are disproportionately affected by pollutants with an environmental justice focus in Atlanta Metropolitan.

The study was conducted through the following analyses:

(i) Assessing the spatial-temporal variation of sources of contamination in the Upper Chattahoochee River Basin

(ii) Correlating fracture/fault networks with the sources of contamination and distance to the Chattahoochee River’s main trunk and each of its subsidiary watersheds in the Metropolitan area.

(iii) Correlating the spatial distribution of various populations with the sources of contamination in Atlanta metropolitan along the larger Chattahoochee River Basin.

1.3 Research Questions

This research was set to answer the following questions:

1) Is there any spatial-temporal variation of sources of contamination in the Upper Chattahoochee River Basin?
2) Is there any correlation between socioeconomic status and the distribution of sources of contamination in the UCRB around the Atlanta Metropolitan area? In other words: Are sub-populations with a lower socioeconomic status more exposed to a higher number of sources of contamination compared with others with higher socioeconomic status?
3) What is the spatial pattern of the distribution of the contaminants in each sub-watershed and its contribution to the main Chattahoochee River watershed downstream?
4) Is there any correlation between the interconnectivity (intersection density) of the networks of fractures/faults systems and sources of contamination along the Chattahoochee River's main trunk?

2 LITERATURE REVIEW

2.1 GIS and Point and Non-Point Source Pollutions

The U.S. EPA defines non-point source pollution as contaminants of water resources, surface land, and soil that come from many separate sources. Non-point source pollution is diffuse and cannot be materialized in a single point. The U.S. EPA (2012) also attributed non-point source pollutant to "excess fertilizers, herbicides and insecticides from agricultural lands and residential areas; oil, grease, and toxic chemicals from urban runoff and energy production; sediment from improperly managed construction sites, crop and forest lands, and eroding streambanks; salt from irrigation practices and acid drainage from abandoned mines; bacteria and nutrients from livestock, pet wastes, and faulty septic systems".

GIS has been used in the past to examine the spatial distribution of non-point source pollutions. Jabbar and Grote (2019) used a GIS-based geostatistical analysis to examine non-point sources of pollution in agriculture watershed in the Lower Grand River watershed, MO, USA. The authors developed GIS databases providing a spatio-temporal variability of physical, chemical, and biological characteristics of all small watersheds in the Lower Grand River watershed in north-central Missouri and southcentral Iowa. Jabbar and Grote (2019) also used surface water quality parameters in 35 independent sub-watersheds to examine the effect of geology, topography, and land use on the water quality in Midwestern watersheds. The results of these work indicate a significant correlation between geologic and land use characteristics and water quality parameters and show a negative impact of agricultural activities by elevating the amounts of phosphorus and nitrogen in many Midwestern streams and lakes. The work also demonstrated the usefulness of GIS-based statistical modeling techniques in water quality monitoring and locating and mapping of non-source of contamination. He et al (2014) modeled the spatial distributions of nonpoint

source loading potential in the Saginaw Bay Basin, Michigan, USA. The authors use multiple databases of hydrography, soils, agricultural water quality, meteorology, land use, and topography through a GIS-model interface to examine the distribution of source of contamination over time and space. He et al (2014) found that the major part of the total nutrient loading in the watershed is from both point and nonpoint sources. A non-point source has the largest contribution in the nutrient loading among the studied watersheds, especially in the rural watershed.

Land use and land cover such as agriculture, forestry, abandoned mined drainage, roads, highways, bridge, urban areas, wetland, and riparian areas, and hydro-modification, habitat alteration, and marinas and boarding have driving effects in non-point source pollutants. Many studies have shown that land-use change can increase pollution from nonpoint sources, degrading considerable water resources, and generating nutrients in surface flow. Tu (2011) examines the impact of land-use changes in water quality in 43 watersheds in metropolitan Atlanta and its surrounding areas in northern Georgia applying GIS and statistical analyses. The author uses Digital Elevation Models (DEM) to delineate watersheds' boundaries to define sample sites and derive land-use types such as forest, urban land, agriculture land, and wetland for each watershed. Tu (2011) thereafter performs GIS-based statistical analyses to quantify and examine the spatial and temporal relationship between land use and water quality. Although the results of Tu (2011) indicate a significant spatial relationship between water quality and land use, no temporal pattern was revealed by the analyses. According to Tu (2011), a study of long-term change in water quality should consider both natural and anthropogenic factors. Yang et al (2014) examined the effects of land-use changes on nonpoint source pollution in the Three Gorges Reservoir, China. The authors used the Soil and Water Assessment Tool model, an empirical regression equation, and GIS to assess relationships between land-use changes and nonpoint pollutants in the study area. Yang et

al (2014) found that land-use change has a strong driving effect on nonpoint pollutants in the study area. The result also showed a significant relationship between land-use change and nonpoint pollutants. Cressie and Majure (1998) developed a novel GIS statistical modeling technique to examine livestock waste in streams of the upper North Bosque watershed, Texas. The author collected daily data for 15 days from 17 stream monitoring sites to measure and predict the variation of nitrate concentration over time at all stream locations. According to Cressie and Majure (1998), the spatio-temporal model presented is an efficient modeling technique allowing the prediction of contaminant concentrations in space and time with a known confidence level and presents a novel approach to GIS in solving a prediction problem.

The need to apply modern approaches and tools to monitor and inventory point source pollution, and identify potential pathways for contaminant transport from point source pollution has been emphasized over the last decade to reduce the potential risks to surface and groundwater contaminations (Machiwal and Jha, 2010). The U.S. EPA (2012) defines point source pollution as "any discernible, confined and discrete conveyance, including but not limited to any pipe, ditch, channel, tunnel, conduit, well, discrete fissure, container, rolling stock, concentrated animal feeding operation, or vessel or other floating craft, from which pollutants are or may be discharged". GIS-based geostatistical modeling techniques and multivariate statistical analyses have been used in the past to study surface and groundwater contamination. Machiwal and Jha (2015) used multivariate statistical analyses and GIS-based geostatistical modeling techniques to study contaminant sources in a fractured rock aquifer system in India. The authors explored fifteen groundwater quality parameters using the principal component analysis and geostatistical modeling combined to identify sources of groundwater contaminants. Results of Machiwal and Jha (2015) revealed a correlation between rainfall and groundwater quality, and control of

groundwater contamination by the geology of the study area and anthropogenic processes. Jelks et al (2018) developed a participatory mapping approach in the Proctor Creek Watershed (Atlanta, Georgia) through a community-based knowledge to emphasize the importance of involving residents in the environmental hazardous studies. The approach allows Proctor Creek Watershed resident to use their knowledge and live experience to analyze and document the environmental stressors in their community through a designed mobile application collecting the resulted data associated with these stressors. According to Jelks et al (2018), knowledge from communities living in degraded environment areas can contribute to scientific inquiry, help advance environmental justice, and positively influence environmental remediation process and policy change. Jelks et al (2018) study has contributed to the environmental hazards' datasets in the Proctor Creek Watershed. Adhikary et al (2015) used a spatio-temporal approach to assess variation in groundwater quality for irrigation in west Delhi, India through a GIS-based multi-criteria system. The authors found that the groundwater in the southern part of the study area is mostly unsustainable, and the western and northern parts were observed to have variable quality.

2.2 DRASTIC Model and Groundwater Contamination

The DRASTIC model is a worldwide-used method to assess aquifer vulnerability to contamination, developed for the United States Environmental Protection Agency by Aller et al in 1987 (Chakraborty, 2007). During the last decade, the need for the application of the modern system and tools to address groundwater contamination issues in the United States has been emphasized. The DRASTIC model combined with GIS is a viable tool for visualizing groundwater potential to pollution through a vulnerability map. GIS was first used to implement the DRASTIC model by Merchant et al (1987) and Martinko et al (1987). Many other studies in the past have used the DRASTIC model combined with GIS to assess groundwater vulnerability. Shirazi et al

(2012) reviewed several papers developing the GIS-based DRASTIC model as a methodology to assess groundwater vulnerability. The authors compared the DRASTIC method with various types of overlay & index methods to assess its ability to identify some research gaps. Shirazi et al (2012) found that the combined GIS and DRASTIC models are more efficient to assess groundwater vulnerability, and can be adopted in different regions such as basaltic, arid, semi-arid, and agricultural. Shirazi et al (2013) examined groundwater vulnerability assessment in the Melaka State of Malaysia using the DRASTIC Model combined with remote sensing and GIS techniques to illustrate the groundwater vulnerability map for the study area. They found two cities of the Melaka State: Jasin, and Alor to be the most vulnerable areas. Chakraborty et al (2007) examined the aquifer vulnerability to pollution in West Bengal, India using DRASTIC Model. The authors' results indicated the presence of arsenic impacting 62% of the vulnerability class area. Akram and Hallaq (2011) used the DRASTIC Model to assess the groundwater vulnerability to contamination in Khanyounis governorate, Palestine. The authors used ArcGIS 9.3 software and the hydrologic characteristic of the study area to develop a vulnerability map. These authors indicated the soil media as the most significant parameter influencing the pollution of the Khanyounis governorate groundwater. Jang et al (2017) applied the DRASTIC model to assess aquifer vulnerability to contamination for sustainable groundwater management and protection. The paper also emphasized the efficacy of using a binary classifier to calibrate DRASTIC weights with a genetic algorithm (Bi-GA) to assess aquifer vulnerability to contamination. Jang et al (2017) results indicated that the proposed approach is a viable tool that may apply to any area for groundwater management efforts.

Other studies combine the standard DRASTIC model with land use/land cover (LULC) data and/or lineament density map to develop a new model for assessing groundwater vulnerability

to contamination called the "modified DRASTIC model". For example, Abdulla et al. (2014) developed a modified DRASTIC model by associating the generic DRASTIC model with land use activities and lineament density to assess groundwater vulnerability in Amman-Zerqa Basin (Jordan River). Abdulla et al (2014)'s results present the modified DRASTIC model as a viable tool for groundwater vulnerability assessment to various types of pollution. The paper also emphasizes the importance of considering land-use factor when changing human or agricultural activity patterns in a basin, and the precision of the modified DRASTIC model by comparing high contaminated areas with nitrate concentration level data which show a linear relationship. Singh et al (2015) examine various models including the modified-DRASTIC model named DRASTICA to evaluate groundwater vulnerability to pollution in an urbanized environment in Lucknow, India. Their method applies an innovative methodology to assess the influence of human activities using satellite observations of night-light and land-use/land cover surrounding the urbanized area in Lucknow, India. Singh et al (2015), results proved the proposed DRASTICA model as an efficient method for assessing groundwater vulnerability in an urbanized environment. By verifying the results with nitrate concentration in groundwater, the authors found the model to yield a better result than the standard DRASTIC model. Through a sensitivity analysis, they also found that anthropogenic impact and depth to the water table have a significant impact on the model. Ahmad and Akihiko (2008) examined the relationship between the DRASTIC model and human activity impact indices to assess groundwater vulnerability to contamination within the Dead Sea groundwater basin in Jordan. The results indicated that the depth to the water table and hydraulic conductivity have a low impact on the model compared to, the vadose zone, aquifer media, and recharge parameters that significantly impact the DRASTIC model. Ahmad and Akihiko's (2008) results also showed an impact of human activity on groundwater quality, as it increases the

pollution risk. The authors verified the results with the nitrate concentration map, which shows a good relationship.

2.3 GIS and Environment Justice Assessment

In addition to providing a variety of qualitative and quantitative tools for the visualization of environmental situations, GIS is a helpful tool for evaluating environmental justice and informing the general public about contamination. Spatial dispersion of low-income and minority populations, and quantitative analysis of racial, ethnic, and economic data (income, ownership) can be studied and performed through different techniques in GIS (Zimmerman, 1993). The availability of demographic data in digital format and at different spatial levels, e.g., block, census tract, zip code, and county, and the increasing computational power have extended the application of GIS to the assessment of environmental justice (Burke et al., 1993). A few studies in the past have correlated the spatial distribution of subsets of a population-based on income level, race, and ethnic origin to the distribution of hazardous waste sites to analyze environmental justice impacts. MacDonald et al (2014) correlated race with water access in North Carolina. The authors determined the percentage of residences with municipal water service in Wake County, North Carolina, using tax data and logistic regression methods. The motivation behind their research was based on the fact that African American communities on the fringes of cities and towns in North Carolina have been systematically denied access to municipal drinking water service. MacDonald et al (2014) found that an increase of 10% in African American population proportion within a census block increased by 3.8% the odds of exclusion from municipal water service. Bullard et al (2007) examined toxic wastes and race in the United States and produced the report: "Racial and Socio-Economic Characteristics of Communities with Hazardous Waste Sites". They found race to be more efficient than household income for predicting the location of hazardous waste facilities

in the United States. Pasetto et al (2019) reviewed 14 articles in the procedural environmental justice in sites contaminated by hazardous waste from industries in the World Health Organization European Region. The authors found that, except for the UK, the countries in the WHO European Region are in their early stages in terms of environmental and health inequalities studies and the generation of their mechanisms in areas affected by hazardous waste from industries. Khabo-Mmekoa and Momba (2019) evaluate the social disparities between rural and urban areas in Ugu District, South Africa. The authors used water quality data and social-economic data to evaluate the social disparities in terms of the provision of safe drinking water, housing patterns, access to sanitation facilities, and health issue related to diarrheal episodes. Khabo-Mmekoa and Momba (2019) result revealed a significant social disparity between rural and urban areas in terms of water supply and quality, and a high level of E. Coli contamination in the stored water used by the rural community of Ugu District. Bolin et al (2000) used the U.S. EPA Toxic Release Inventory (TRI) to perform a spatial distribution analysis of industrial facilities releasing toxic substances in Phoenix, Arizona. They found a clear pattern of environmental inequity in Phoenix and unequal distribution of risk.

Kumar (2002) examined various methodologies that evaluate the risk of the disproportionate burden to communities through a survey of the literature and public institutions concerning the unique character and composition of New England. The author used specific variables such as ethnicity, poverty, and population density to determine threshold/reference value and establish a ranking system along with investigating spatial clustering into combined criteria. Kumar (2002) made several recommendations to the EPA New England regional office on how to improve their demographic mapping system with various methods of analysis. Park and Kwan (2017) studied the limitations of traditional residence-based approaches in terms of examining the

relation between socioeconomic or racial/ethnic segregation and unequal environmental exposure through a review of the relevant literature. The authors also examined the importance of using fine-scale spatiotemporal approaches in assessing environmental exposure in environmental justice research. Park and Kwan's (2017) result reveals that future research needs to assess environmental exposure at a high spatiotemporal resolution and consider various geographic and temporal contexts i.e., beyond residential segregation. According to the authors, this approach can significantly expand the scope of environmental justice research. Schaider et al (2019) examined environmental justice and drinking water quality to identify socioeconomic disparities in nitrate levels in U.S. drinking water. The researchers used EPA's Safe Drinking Water Information System (SDWIS) along with nitrate data from 2010 and city- and county-level demographic data to identify socioeconomic disparities in nitrate levels. The authors also applied multivariable regression analyses at national and regional scales to study disparities at large scale. The Schaider et al (2019) results reveal significant disparities in term of drinking water quality as far as nitrate levels in U.S. According to the authors, between 2010 and 2014, 5.6 million Americans used Community Water System (CWS) with an average nitrate concentration larger or equal at 5 mg/L NO3-N. Water provided by each system to the percent of Hispanic residents is significantly associated with nitrate, exceeded 5 mg/L nearly three times as often as CWSs serving the lowest quartile. Schaider et al (2019) study also shows a significant association between the extent of agricultural land use and groundwater nitrate concentration.

3 METHODS AND PROCEDURES

3.1 General area description

3.1.1 Geographical context

The Chattahoochee River has its source in the southeast corner of Union County in the southern Appalachian Mountains. The river runs about 434 miles and flows southwesterly through the Atlanta metropolitan area and Alabama before terminating in Lake Seminole in the Georgia–Florida border (Cook, 2018). At the Georgia-Florida border, the Chattahoochee River joins with the Flint River where the name changes to the Apalachicola River in Florida. The entire drainage basin is often named Apalachicola-Chattahoochee-Flint (ACT) basin (Cook, 2018). The Chattahoochee River is the most heavily used water resource for the drinking water of Georgia (an integral facet of the state of Georgia and the city of Atlanta), providing more than 70% of metro-Atlanta's water needs (EPD, 1997). Thirteen dams and three lock-and-dam facilities that regulate and control the flow of the River over most of the portion of its length are responsible for generating hydropower and electricity (Cook, 2018). In the 1950s, the U.S. Army Corps of Engineers impounded the Chattahoochee River at Buford Dam to create Lake Lanier. Lake Lanier and the Chattahoochee River provide 72% of metro Atlanta's water supply and assimilate a large amount of major wastewater treatment plant discharge (EPD, 1997).

Figure 3-1 Map of the Apalachicola-Chattahoochee River Basin (Riverkeeper

The Upper Chattahoochee River (UCR) Basin flows southwest to the confluence of the Chattahoochee River with Peachtree Creek. Its headwaters are located in the Blue Ridge Mountains northeast of the Metro Water District, and approximately 43 percent (680 square miles) of this UCR Basin is located upstream of the Metro Water District. Through the center of the Metro Water District (about 40 miles wide), the UCR occupies a relatively narrow corridor, which starts in the northeast corner and extends to the southwest corner (USGS, 2017)**.** The UCR forms the largest river basin within the Metro Water District when combined with the Middle Chattahoochee River. It covers 1,823 square miles. The Metro Water District-portion of the Upper Chattahoochee River Basin incorporates portions of 29 cities and 7 counties, including Cherokee, Cobb, DeKalb,

Forsyth, Fulton, Gwinnett and Hall. The City of Brookhaven in DeKalb County, the City of Peachtree Corners in Gwinnett County, 35 percent of the City of Atlanta, and all of northern Fulton County are now incorporated within the Upper Chattahoochee River Basin (Metro Water District, 2002)

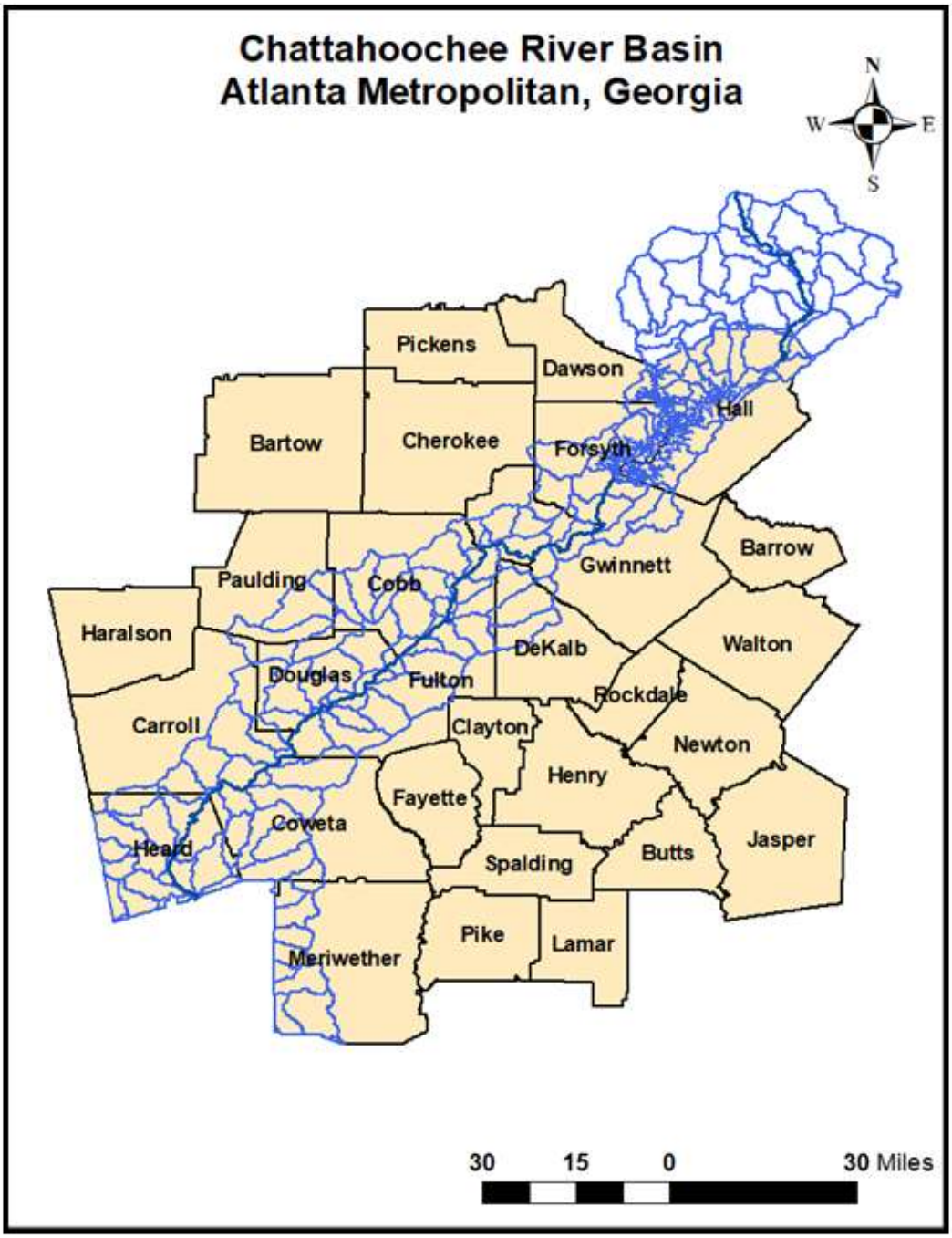

Figure 3-2 Chattahoochee River Basin across Atlanta metropolitan

3.1.2 Geological and hydrogeological setting

The geology of Georgia is made up of five distinct physiographic provinces**.** From the northwest corner of Georgia to the southeast, these are the Appalachian Plateau, Valley and Ridge region, Blue Ridge, Piedmont, and Coastal Plain. These geologic regions are distinct based on their topography, structure, and rock type, and how they weather and erode (Edwards et al., 2013). The study area is entirely within the Piedmont province and includes portions of the Gainesville Ridge, Central Highlands, and the Winder Slope physiographic districts. The Piedmont province (where the Chattahoochee River is entirely located) contains a series of rolling hills and occasional isolated mountains, and lies between the north Georgia and the Coastal Plain. The Piedmont province takes up approximately 30 percent of Georgia (second-largest geographical region after the Coastal Plain) and contains the highest population (Edwards et al., 2013). It has the oldest rocks and the highest mountains in Georgia (above 4000 feet) along with the Blue Ridge. The region is underlain by deformed metamorphic and igneous rocks (crystalline) dated late Precambrian and late Permian age, including granite, gneiss, schist, amphibolite, and migmatite (Gordon and Painter, 2018).

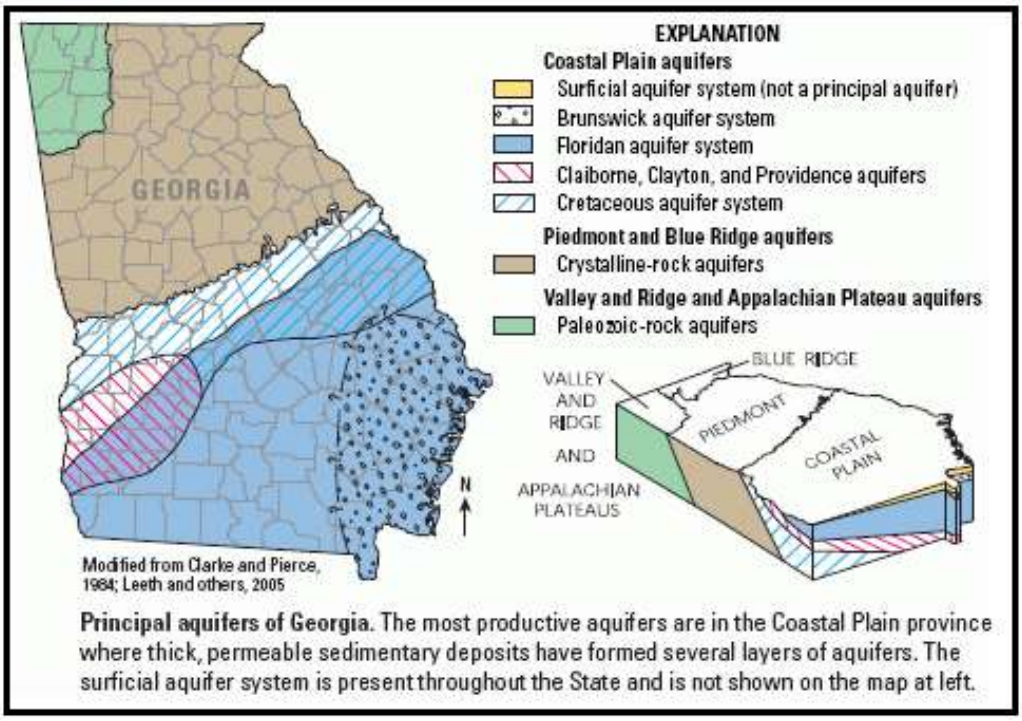

Figure 3-3 Map of Georgia Primary Aquifers (USGS, 1997, modified)

Piedmont takes up most of northern Georgia above the fault line and presents features like Stone Mountain and the Brevard Fault zone. Unlike the Valley and Ridge sediments, geologic structures of Piedmont rocks such as fold and fault formed deep inside the mountain belt, and several mafic dikes intruded in this region during the Mesozoic and Cenozoic Eras. In Georgia, the Brevard Fault zone runs parallel to the Chattahoochee River as a hydraulic control and its rocks are deeply sheared and fractured. Such rocks include schists, mylonite, and gneiss (Edwards et al., 2013). The aquifer in the study area is in crystalline rock (igneous, metamorphic), and is overlain by a layer of unconsolidated rocky material (regolith). Such rocks and fractures in the study area make up the available aquifer porosity and control the flow of water and transport of pollutants and groundwater recharge (USGS, 2017).

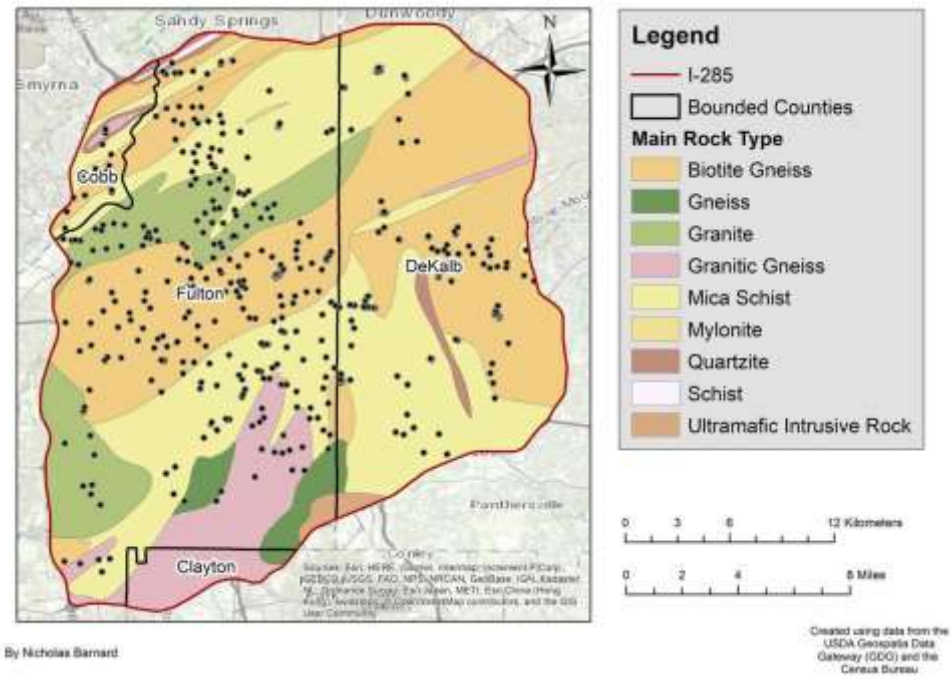

Figure 3-4 Atlanta Underlying Bedrock Geology (USGS, 1997)

3.1.3 Soils of the study area

The soil types in the study area are described by four soil associations: Cecil-Madison-Pacolet, Madison-Davidson-Pacolet, Riverview-Chewacla-Cartecay, and the "urban" soils starting in North Fulton County. The first two types of soil are well-drained, highly weathered, and the most abundant in the study area. These types are associated with moderate rolling hills (Murphy, 1979). The Riverview-Chewacla-Cartecay association is less well-drained and is located along major river banks such as the lower half of the Chattahoochee River. The "urban" soils are highly disturbed and compacted. Hence, they are poorly-drained and are less feasible for infiltration (Thomas and Tate, 1973). Soils of the study area are acidic and nutrient-poor with a typical pH of around 4.7, and thickness between 3 and 6 feet. The texture ranges from sandy to loamy depending on local topography and hydrology (Edwards, 2013). The soil mineralogy depends on the bedrock material, and is extremely variable within the urban environment. The primary mineralogy of the

soils is quartz, kaolin, iron oxides, and vermiculite. When chemical weathering occurs, the native soils of the study area are heterogeneously weathered from quartzite, gneiss, mica schist, ultramafic intrusions, ultra-mafic dikes, and mylonite (Gore and Witherspoon, 2008).

3.2 Data collection

The data for this project, retrieved from multiple sources, include hydrology, geology, and hydrochemical types collected from the Upper Chattahoochee River Basin (UCRB). These include spatial and temporal data from the National Water Information System (USGS water resources, https://waterdata.usgs.gov/nwis/qw) and the National Oceanic and Atmospheric Agency (NOAA), as well as the spatial extent of the UCRB (.shp file) and its sub-watersheds in the study area (around the Atlanta Metropolitan area). Hydrochemical data include physical and chemical characteristics of surface water parameters (drinking water quality). Data and information, acquired in spatial and geographic formats, include maps, shapefiles, Excel files, geodatabase files, and charts. The USGS National Water Information System (NWIS) includes more than 850,000 station years of time-series data and supports the acquisition, processing, and storage of water data. Such data describe reservoir and lake levels, stream levels, streamflow, surface-water quality, and rainfall (USGS, 2020).

The project also applied spatial and temporal data related to sources of pollution of all kinds in the study area. This includes sources such as farms, chicken farms, factories, storages, airports, gas stations, sewers, waste sites. These time-series data were gathered from the U.S. EPA Toxics Release Inventory (TRI) program that provides resources about toxic chemical releases reported by industrial and federal facilities since 1987 (https://www.epa.gov/toxics-release-inventory-tri-program/tri-listed-chemicals). Through the TRI Program, U.S. facilities must annually report the amount of chemicals released to the environment and/or recycled, recovered,

and treated. EPA compiles the information in the TRI and makes them available through different online tools**.** Data for the sources of contamination were mainly downloaded from this website. The time-series data range from 2000 to 2019. Data and information included maps, shapefiles, Excel files, geodatabase files, and charts.

Comprehensive population data, including the spatial distribution of subgroups, i.e., different people **(**with all attributes such as age, income, race, sex etc., that distinguish them from each other**)** living in the study area. The population data were obtained from the US Census Bureau (US census) and the Atlanta Regional Commission (ARC). The US Census Bureau (https://www.census.gov/programs-surveys/geography/geographies/mapping-files.2018.html) produces yearly population estimates at the state level for the USA while the ARC makes yearly population estimates for the 10-county Atlanta region (https://opendata.atlantaregional.com/). These data are tabulated based on race, ethnicity, income, age, gender, etc. and are time series.

Landsat 8 image and ASTER-DEM from May 2019 of the study area are from the USGS Earth Explorer website. The USGS Earth Explorer (https://earthexplorer.usgs.gov/) supports geospatial datasets from extensive dataset such as Landsat satellite imagery, Radar data, UAS data, digital line graphs, digital elevation model data, aerial photos, Sentinel satellite data, IKONOS and OrbView3, land cover data, digital map data, and many other datasets (USGS**)**. The day for each image is specified depending on how the atmospheric condition was in the Atlanta region during that month (cloudy, cloud-free, etc.). The imaging times were selected in early summer (May) to reduce the influence of the cloud and other atmospheric factors on the images.

The project also involved using land use/land cover (LULC) data. The LULC data was produced from the unsupervised classification of Landsat 8.

Fracture/fault data (lineament) were obtained by extraction from Landsat 8 using Geomatica software and ArcGIS. This is an automatic extraction allowing to get lineament data (lineament maps) and its attributes (coordinates of their center point, length).

Surface quality parameters used data on Ca, Mg, Na, K, Fe, SO4, Cl, NO3, SiO2, EC, pH, P, Cu, Cr, Ni, Mn, Pb, Zn in the study area. These data are available on the USGS National Water Information System website (https://waterdata.usgs.gov/nwis/qw).

3.3 Methods

3.3.1 Mann–Kendall test and Sen's slope estimation method

To detect and quantify trends in water quality parameters, Mann–Kendall test, and Sen's slope estimation method (refer to as Sen's slope test) were applied respectively in this study. The two general approaches for trend detection are parametric method and nonparametric method. The parametric method is used when the mean more precisely represents the center of the distribution of the data, and the sample size is large enough. The nonparametric method is used if the median more accurately represents the center of the distribution of the data. Thus, the parametric method is used only when the data are independent and normally distributed (Machiwal and al., 2012). In this study, a nonparametric test is used to detect the existence of a long-term trend in water quality parameters. The commonly used and preferred nonparametric trend detection methods in hydrology are Spearman Rank Order Correlation test, Kendall's Rank Correlation test, and Mann–Kendall test (Machiwal and Jha 2012; Shahin et al., 1993; Kanji, 2001; Machiwal et Jha, 2015; Kumar, 2003; Zipper et al., 1998**).** The Mann–Kendall test were performed in this study for the detection of a trend and correlation among surface quality parameters (Ca, Mg, Na, K, Fe, SO4, Cl, NO3, SiO2, EC, pH, P, Cu, Cr, Ni, Mn, Pb, Zn) using two decades data (2000 to 2019) of 250

surface water sample sites. The Mann–Kendall analyses were conducted using SPSS and Microsoft Excel.

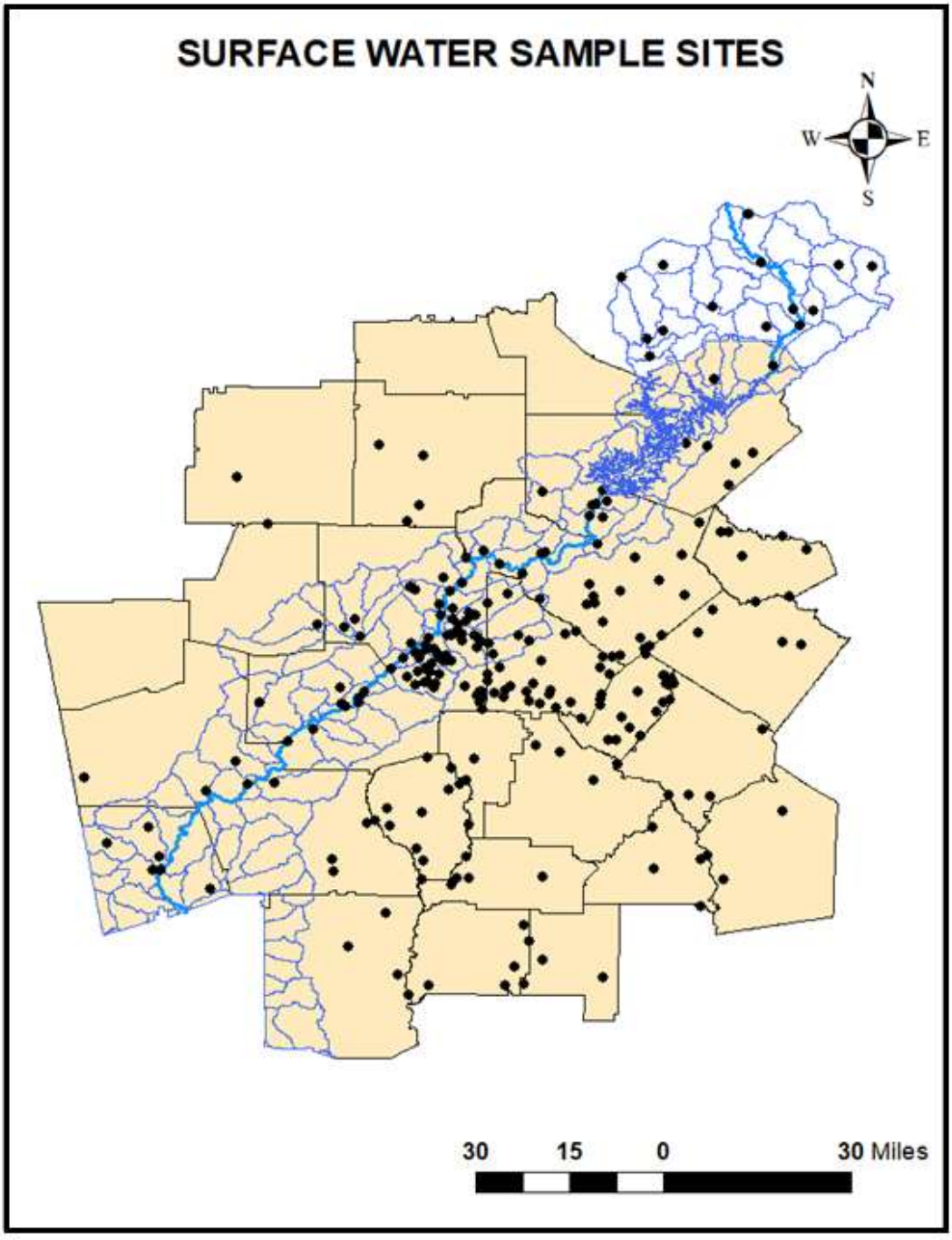

Figure 3-5 Surface Water Sample Sites

The Sen's slope estimation method was then used to quantify trends in all groundwater quality parameters. It is the most popular nonparametric technique for estimating a linear trend in the water quality time series of equally spaced data i.e., the slope of a regression line that fits a set of (x, y) data elements (Sen, 1968). The Sen's slope is an extension of the method developed by Theil in 1950, and the approach is not valid when the data elements don't fit a straight line (Theil, 1950). Thus**,** positive and negative groundwater quality trends were quantified using the following slope estimation equation (Sen, 1968):

$$\beta_k = \text{Median}\left(\frac{x_{ik} - x_{jk}}{i - j}\right) \quad \text{for all } i < j$$

Where β_k = slope between x_{ik} and x_{jk}; x_{ik} = data measurement at time i; x_{jk} = data measurement at time j; and k = site. The positive value of β_k refers to an upward trend and a negative value to a downward trend.

3.3.2 Principal component analysis (PCA)

PCA is a statistical technique applied to a single set of variables to reduce multidimensional datasets to lower dimensions that can be more easily visualized and analyzed (Davis, 2002). PCA is the widely used statistical methods for analysis and ranking of water chemistry (Machiwal and Jha, 2015; Dunteman, 1989; Abdi and Williams, 2010)**.** The purpose of this analysis in this study was to transform the data of each surface water sampling site into a small uncorrelated set of factors called principal components (PCs). The PCs will contain most of the information present in the original surface water dataset with a small loss of total variance. Also, with the help of PCA, the correlation between surface water variables can be detected, which might also describe the contamination process or sources. PCA was performed in this study using the 18-surface water parameter (Ca, Mg, Na, K, Fe, SO4, Cl, NO3, SiO2, EC, pH, P, Cu, Cr, Ni, Mn, Pb, Zn) for 20

years (2000 to 2019). SPSS statistics software was used and the water quality data were standardized by the Z-scale transformation.

The PCA mainly consists of two steps, data standardization, and PC extraction. The range of the initial variables is standardized for an equal contribution of each of them to the analysis. It is important to perform data standardization prior to PCA as any large difference between the ranges of initial variables would result in the dominance of the larger range variables over the variables with small ranges in the analysis (Dunteman, 1989). The next step of the PCA is to compute the covariance matrix to identify any relationship between variables i.e., how variables of the input dataset are varying from the mean. Thereafter, the principal components are identified, and the less important variables disregarded by extracting the eigenvectors and eigenvalues of the correlation matrix. Eigenvectors and their corresponding eigenvalues are the special set of scalars that need to be set in a descending order to find the principal components in order of significance (Davis, 2002). Furthermore, Kaiser Normalization Criterion was also used to determine the number of PCs to retain from extraction (Kaiser, 1958). The PCs that contain most of the information present in the original surface water quality data with a small loss in total variance were considered for further analysis.

3.3.3 Spatial pattern analysis of contaminant sources (K-Function)

As stated in the thesis introduction, analyzing the spatial distribution of contamination sources in the Atlanta metro area is one of the main objectives. The aim of applying data mining and point pattern analysis is to extract patterns from data and transform them into information. Point pattern analysis is the evaluation of the spatial arrangements (patterns) of a set of points in space (Marcom et al., 2013). Point distribution can show a clustered pattern, dispersed pattern, or random pattern. The most widely used point pattern analysis methods are Quadrat Analysis,

Nearest Neighbor Analysis, Ripley's K-function, and Spatial Autocorrelation Coefficient. Theoretical detail on how these methods work is omitted here to keep the thesis in an adequate length. In this study, Ripley's K-function statistic was performed to describe how point patterns occur in the study area over two decades (2000-2019), especially in 2000, 2003, 2006, 2009, 2012, 2015, and 2019 using ArcGIS. Ripley's K-function is a spatial analysis method to analyze clustering or dispersion over a range of distances. It examines how spatial clustering changes when the neighborhood size changes. Ripley's K-function statistic is the commonly used tool among the point pattern analysis methods to characterize the spatial structure of a point set. Theoretical details on Ripley's K- function can be found in (DIXON, 2002; Marcom et al., 2013).

Furthermore, the result from the above analysis (sources of contamination) was correlated to the spatial distribution of all groups of people in the study area. Sources of pollution distribution were correlated with socioeconomic status (race, income, sex and age) and adjacency to contamination sites to examine the disproportionality of hazardous exposure in the study area. Maps and charts were created to visualize this correlation.

3.3.4 Lineament extraction and analysis

The aim of extracting lineament information from Landsat 8 image and ASTER-DEM was to generate the lineament map (from the fracture/fault data). The lineament map as a thematic map includes the lineament map, lineament length density map, lineament counts density map, and lineament cross-point density map. Such lineament maps help to contour the intersection points of these lineaments to find high-density areas of potential groundwater recharge from surface and soil waters, especially where contamination sources are located. The map also allows creating rose diagrams from the fracture data to plot the orientation of the lineaments and get a sense of possible surface water and groundwater interaction. Lineament extraction is an application of remote

sensing to geology. It is useful for geological analysis and oil exploration and constitutes an interesting approach in geological mapping and mineral exploration (Sander et al., 1997). The process includes automatic extraction from satellite imagery of lineament information such as orientation and other attributes (e.g., coordinates of their center point, length). Lineaments, as long linear features or patterns on Earth surface, are mapped on satellite imageries from areas with various geomorphologic and/or tectonic structures. They reflect the geological structures such as faults or zones of fractures (Manjare, 2013). However, the real definition or meaning of lineament is still questionable. Geological lineament form as a result of geological processes (fracturing, erosion) and as such must be discriminated from other artificial, man-made or imaging artifact linear features. Therefore, lineament maps should be carefully interpreted by geologists. Richards (2000) and O'Leary (1976) definition of lineament is the widely accepted one, and describe them as linear topographical feature or zones of structural weakness (fractures, faults).

In this study, an automatic lineament extraction system from a Landsat 8 image and an ASTER-DEM was performed using Erdas Imagine, PCI Geomatica software, ArcGIS, and Rockwork 16.

The following main steps were followed to perform the automatic lineament extraction:

- Step 1 consists of using Erdas imagine to perform a principal component analysis (PCA) on the 8-bit grayscale image Landsat 8 image (spatial resolution of 15 m). The resulted principal component image (PC1) of the Landsat 8 pansharpened reflected bands was only considered for the extraction. The PC1 carries out most information and is suitable for lineament extraction purposes.
- Step 2 involved using the LINE module from the PCI Geomatica software to extract linear features from the PC1 generated from Erdas Imagine and record the polylines in a vector

layer. The LINE module extracts lineaments from any singles 8-bit image in three steps: edge detection, thresholding, and curve extraction. Details of these three steps are omitted here to avoid the excessive length of the thesis and can be found in (Prasad et al., 2013). It is important to determine the most accurate parameter of LINE for the best reliable results before the extraction.

- Step 3, the output of the LINE (extracted lineaments) was imported to ArcGIS software for analysis. The ArcGIS software handles the extracted lineaments through three sub-steps: splitting the compound line into simple lines, editing lineament attributes, and exporting lineament as a CAD file. Finally, the exported lineament CAD file was processed to determine the trend of the lineament and generate the rose diagram using Rockworks.

Furthermore, the resulted lineament maps were also used to perform several correlations to measure the dependence of the variables on each other to identify the most important variables that control the spatial and temporal distribution of the contaminants. This includes correlation of the interconnectivity (intersection) of the fractures with sources of contamination (as potential points of recharge for groundwater and point of input of contaminants).

4 RESULTS

4.1 Spatio-Temporal Variations of Water Quality Parameters

The results of the univariate analysis (mean, standard deviation, minimum, and maximum) using 250 surface water quality sample sites for 20 years (2000 to 2019) are shown in Table 4.1. Table 4.1 presents the average yearly data of selected parameters (Ca, Mg, Na, K, Fe, SO_4, Cl, NO_3, SiO_2, EC, pH, P, Cu, Cr, Ni, Mn, Pb, Zn) that were measured in 250 stations across the Atlanta metro in 2000, 2003, 2006, 2009, 2012, 2015, and 2019. It is important to note that data from only one station was available for parameters Na, K, Fe, SO_4, Cl, Cr, Ni, Mn in 2019. Thus, the annual mean values for these parameters were estimated based on the temporal trend and defined pattern of change in the values of the missing parameters. The average values of the missing parameters for 2000, 2003, 2006, 2012, and 2015 were plotted to "extrapolate" an estimated average value for 2019.

Box and whisker plots depicting the variation of 18 surface water quality parameters for 20 years (2000 to 2019) are shown in Figure 4.1. As shown in Table 4.1 and Figure 4.1, there is a temporal variation in the water quality parameters across the Atlanta metro around the Chattahoochee River. Parameters such as Ca, Mg, Fe, SiO_2, NO_3, and Cl present a relatively large length of boxes and whiskers compared to other parameters. However, the highest length of boxes and whiskers were found in the case of Fe and Cl, indicating large spatio-temporal variations.

Table 4-1 Univariate analysis of surface water quality parameters in 2000, 20003, 2006, 2012, 2015, and 2019

	Ca	Mg	Na	K	Fe	SO4	Cl	NO3	SiO2	EC	pH	P	Cu	Cr	Ni	Mn	Pb	Zn
2000																		
Mean	6.69	1.86	9.19	2.36	3.63	5.63	6.82	0.62	9.20	0.10	6.90	0.06	0.0022	0.0014	0.0014	0.2929	0.0020	0.0144
Std. Deviation	4.93	1.49	9.07	1.92	5.01	6.57	5.25	0.65	0.28	0.09	0.33	0.10	0.0035	0.0010	0.0012	0.1957	0.0028	0.0347
Minimum	0.70	0.50	2.78	1.00	0.12	1.39	2.30	0.02	9.00	0.03	5.80	0.01	0.0010	0.0010	0.0010	0.0370	0.0010	0.0010
Maximum	35.00	14.00	15.60	3.72	12.00	13.20	12.70	4.40	9.40	0.85	8.10	0.66	0.0330	0.0080	0.0110	0.6300	0.0240	0.3100
2003																		
Mean	11.21	2.75	8.22	3.68	0.15	12.28	8.02	0.86	13.07	0.12	6.84	0.08	0.0049	0.0008	0.0023	0.1883	0.0028	0.0503
Std. Deviation	7.66	2.44	11.29	2.10	0.08	17.23	9.28	0.67	5.74	0.11	0.39	0.07	0.0178	0.0002	0.0039	0.3948	0.0133	0.2061
Minimum	2.20	0.51	0.97	1.21	0.10	0.02	0.06	0.04	3.71	0.02	4.60	0.01	0.0002	0.0004	0.0004	0.0088	0.0000	0.0006
Maximum	43.50	18.50	81.50	16.70	0.46	135.00	57.40	3.60	26.20	0.90	7.50	0.46	0.1580	0.0020	0.0234	2.3000	0.1120	1.7100
2006																		
Mean	9.21	2.20	6.39	2.36	0.15	14.45	7.03	0.70	12.94	0.10	7.01	0.08	0.0118	0.0043	0.0018	0.2339	0.0043	0.0504
Std. Deviation	5.01	1.16	2.53	0.55	0.15	13.21	3.00	0.63	5.71	0.07	0.41	0.08	0.0117	0.0055	0.0021	0.2562	0.0062	0.1074
Minimum	2.50	0.66	1.68	1.52	0.03	1.37	1.88	0.00	3.41	0.02	5.50	0.01	0.0004	0.0001	0.0002	0.0161	0.0001	0.0010
Maximum	22.50	4.80	10.10	3.48	0.66	58.30	12.20	4.30	23.60	0.54	8.20	0.32	0.0446	0.0180	0.0094	1.0000	0.0300	0.6980
2009																		
Mean	5.86	1.67	4.26	2.39	0.32	14.00	4.52	0.69	6.87	0.10	6.92	0.10	0.0089	0.0016	0.0034	0.1650	0.0067	0.0809
Std. Deviation	3.31	1.03	3.13	0.46	0.16	24.60	3.31	1.15	5.17	0.06	1.11	0.11	0.0109	0.0004	0.0052	0.3910	0.0062	0.1820
Minimum	3.00	0.75	1.78	1.65	0.02	1.18	2.05	0.02	3.76	0.03	0.06	0.01	0.0024	0.0011	0.0005	0.0020	0.0005	0.0062
Maximum	18.70	5.60	10.40	3.01	0.55	83.30	11.20	7.00	19.50	0.33	7.60	0.60	0.0539	0.0023	0.0140	1.2000	0.0240	0.8790
2012																		
Mean	6.84	2.22	7.57	2.17	0.65	10.47	7.41	0.66	15.12	0.10	6.95	0.09	0.0023	0.0006	0.0018	0.2302	0.0029	0.0283
Std. Deviation	3.34	1.29	4.34	0.73	0.45	15.65	5.05	0.85	7.06	0.07	0.38	0.14	0.0033	0.0010	0.0029	0.2595	0.0044	0.0683
Minimum	1.46	0.70	2.27	1.00	0.06	0.85	1.80	0.01	8.56	0.01	5.80	0.00	0.0001	0.0001	0.0002	0.0363	0.0001	0.0002
Maximum	14.90	6.07	16.10	2.93	1.20	40.50	16.90	4.30	26.00	0.51	7.70	0.96	0.0115	0.0025	0.0076	0.6690	0.0201	0.4190
2015																		
Mean	5.81	2.11	4.92	1.82	0.23	11.91	5.10	0.72	7.88	0.11	7.11	0.05	0.0172	0.0004	0.0024	0.1745	0.0129	0.0597
Std. Deviation	2.12	1.29	2.32	1.01	0.22	13.31	3.90	1.06	2.10	0.11	0.41	0.05	0.0222	0.0001	0.0016	0.0728	0.0272	0.0841
Minimum	1.43	0.75	2.32	0.85	0.07	0.90	1.93	0.04	6.58	0.03	5.80	0.01	0.0015	0.0003	0.0013	0.1230	0.0006	0.0039
Maximum	11.00	6.70	6.80	2.86	0.39	26.70	9.46	6.60	10.30	0.69	8.20	0.25	0.0880	0.0005	0.0035	0.2260	0.1400	0.4300
2019																		
Mean	5.43	2.18	**3.93**	**0.87**	**0.29**	**10.25**	**5.08**	0.52	9.14	0.07	7.04	0.10	0.0166	**0.0010**	**0.0010**	**0.2141**	0.0150	0.0768
Std. Deviation	2.28	0.98						0.62		0.04	0.35	0.07	0.0143				0.0112	0.0461
Minimum	1.20	0.57						0.02	9.14	0.02	6.20	0.02	0.0010				0.0007	0.0034
Maximum	12.00	4.20						3.80	9.14	0.21	8.20	0.26	0.0410				0.0420	0.1600

UNIT: ion concentration (mg/L), pH (Standard Units), EC (S/m)

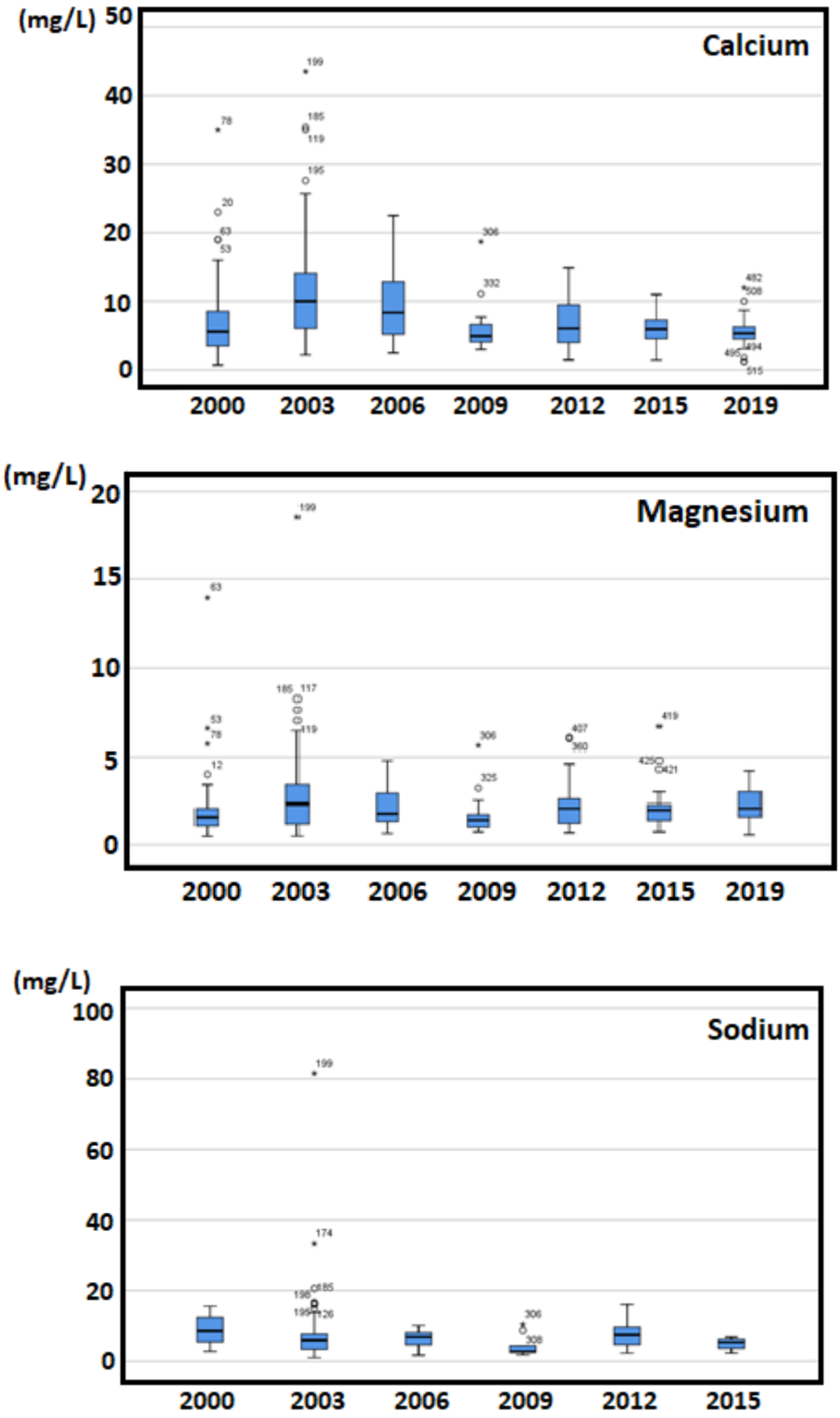

Figure 4-1 Box-whisker plots of surface water quality parameters

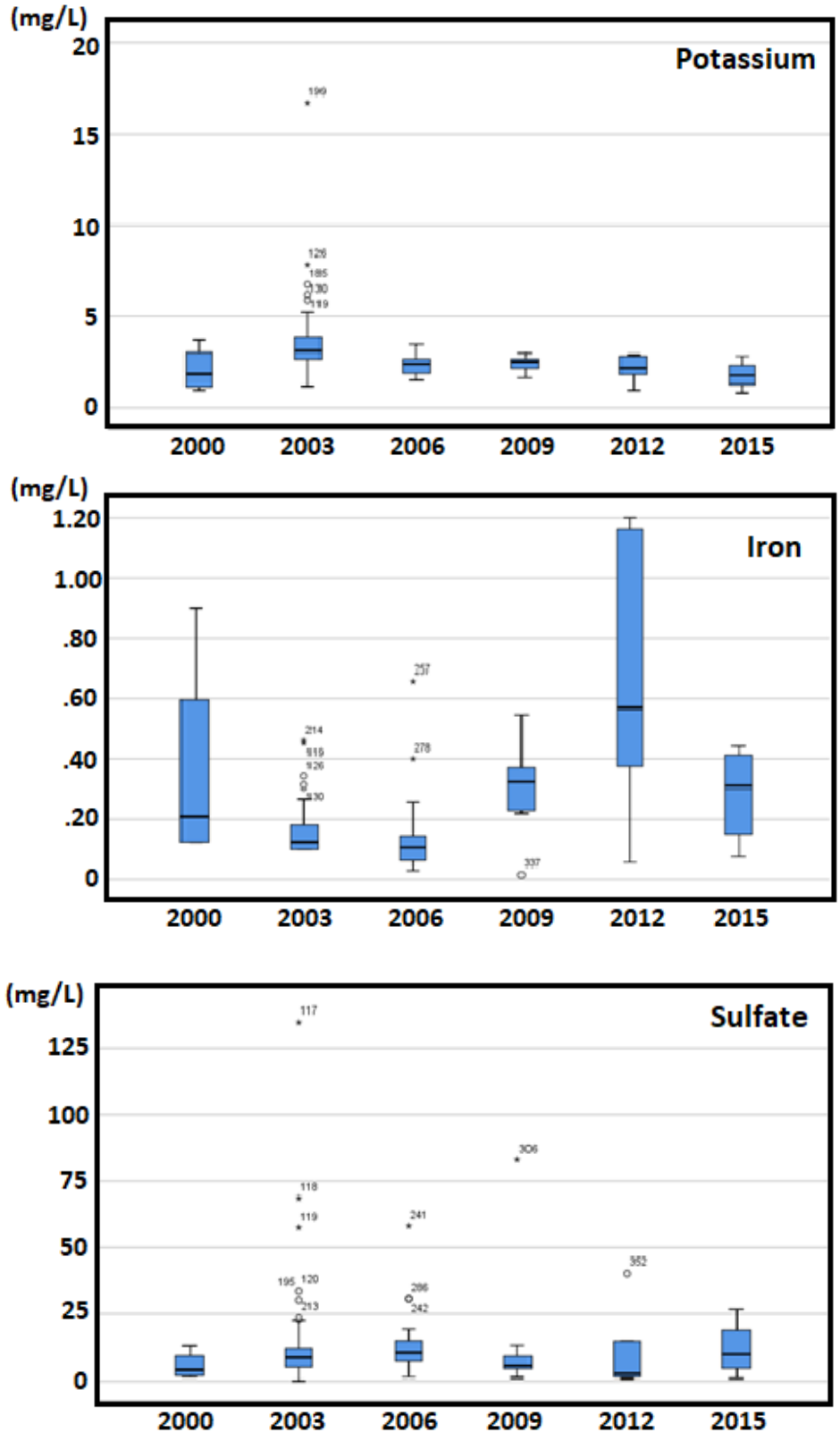

Figure 4.1 (Continued**)**

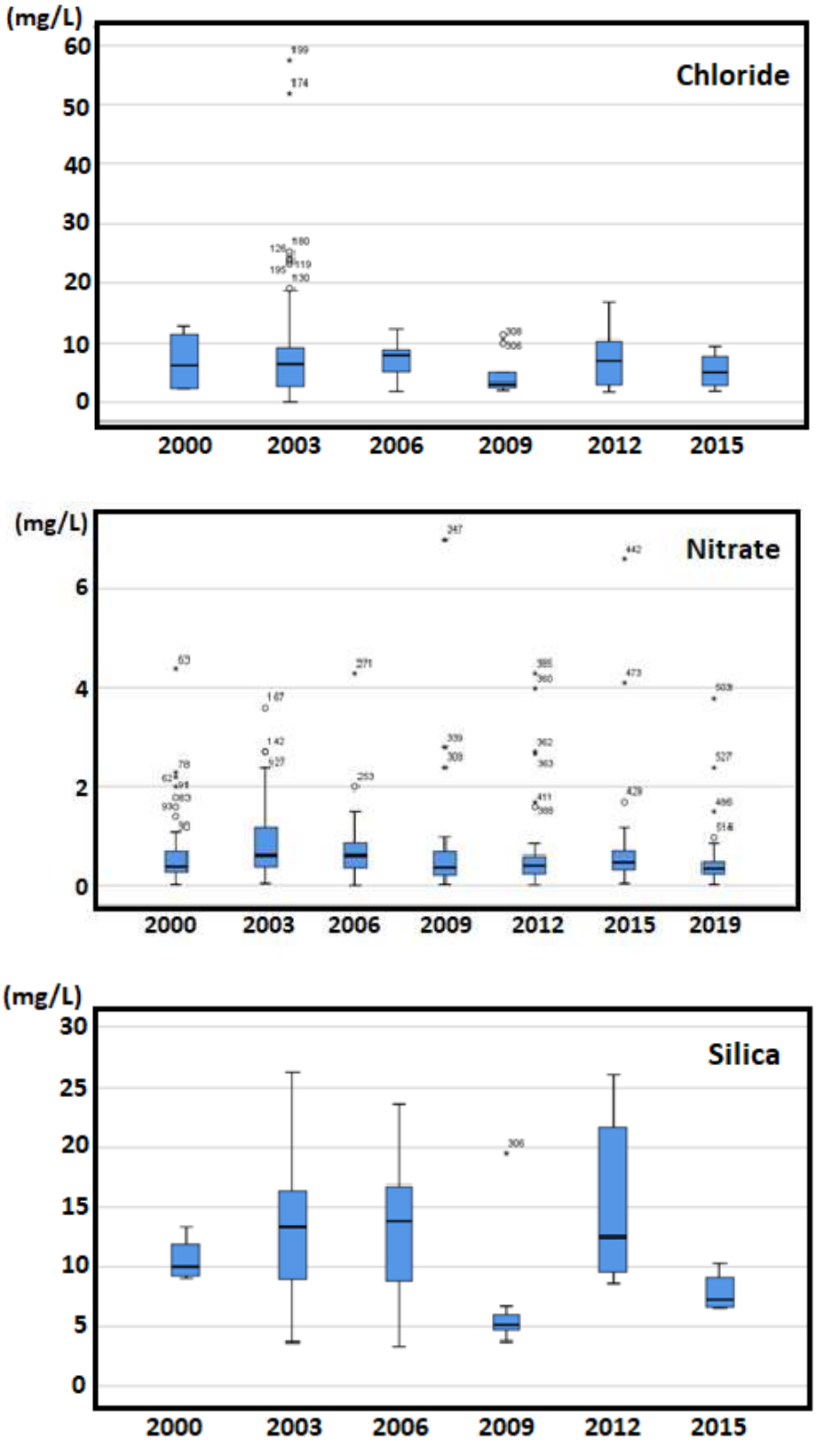

Figure 4.1. (Continued)

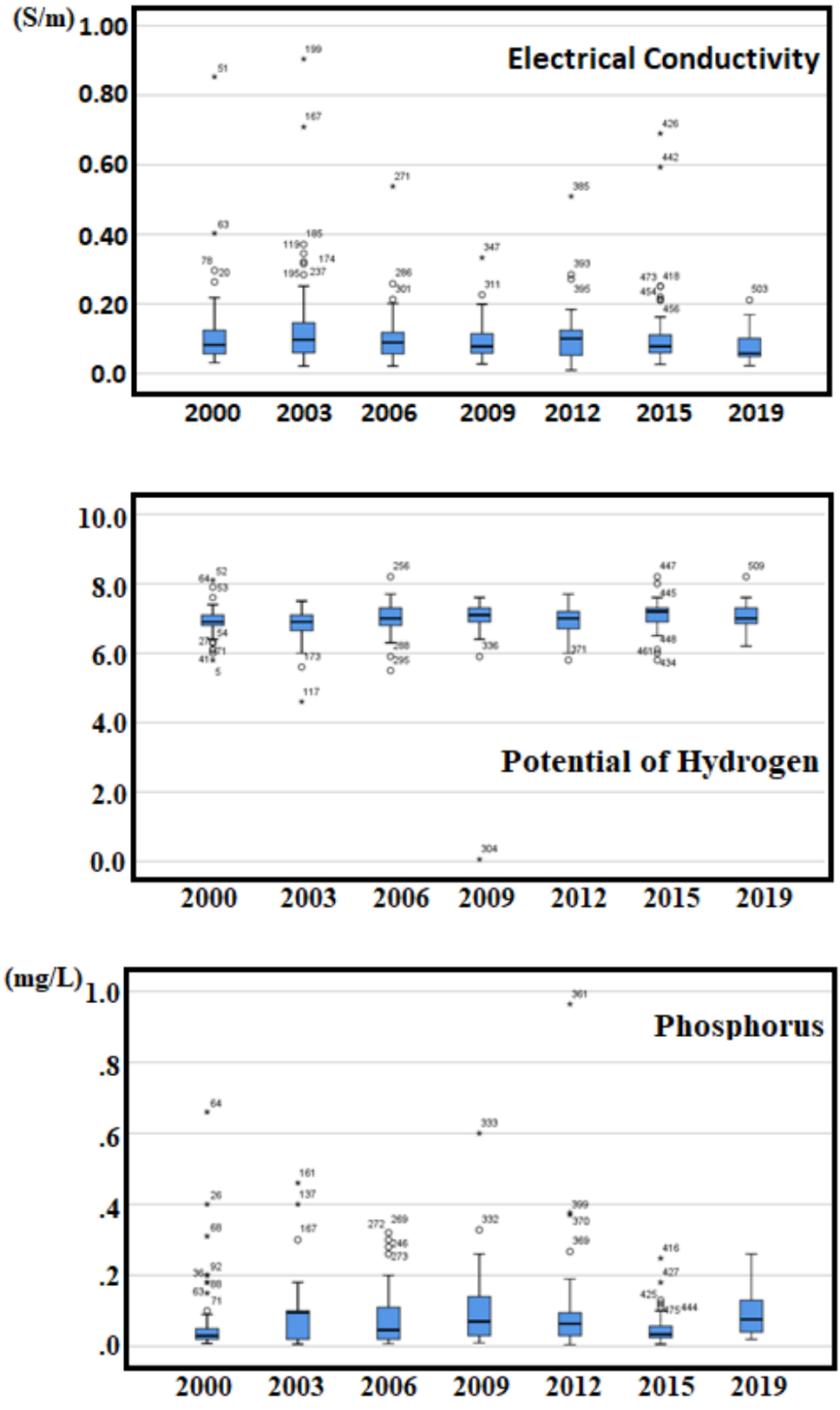

Figure 4.1 (Continued**)**

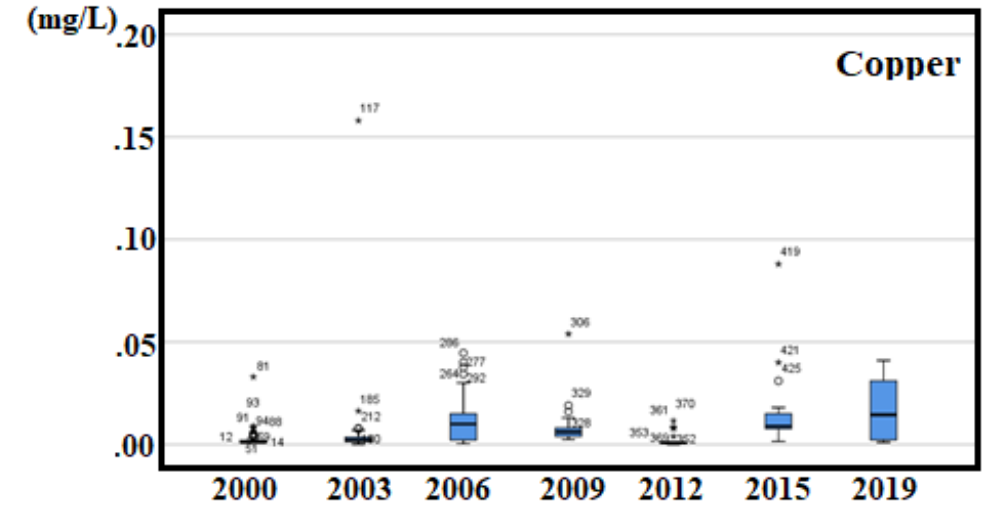

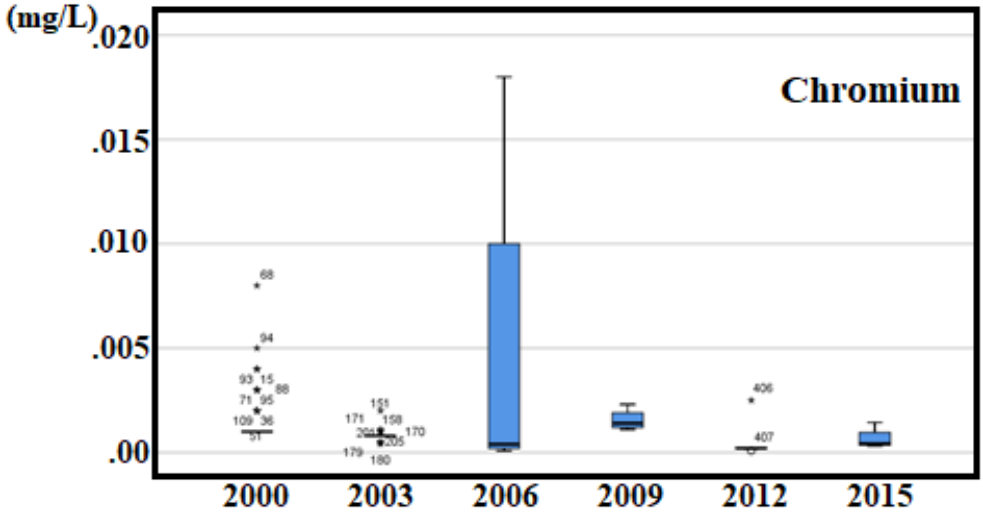

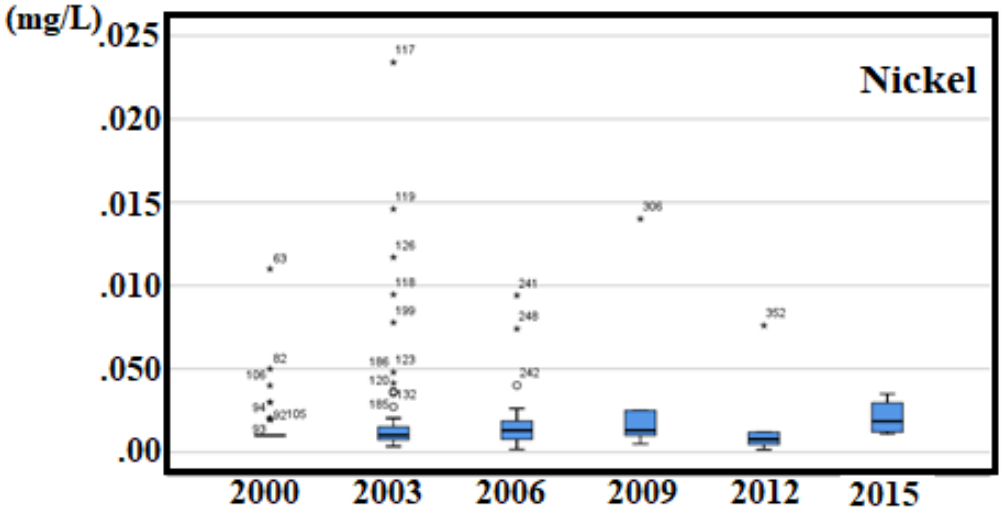

Figure 4.1 (Continued**)**

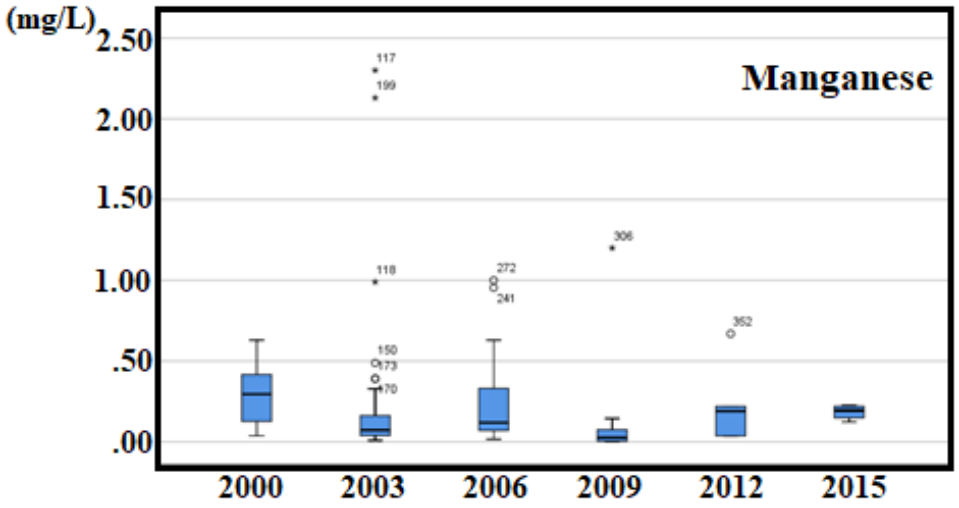

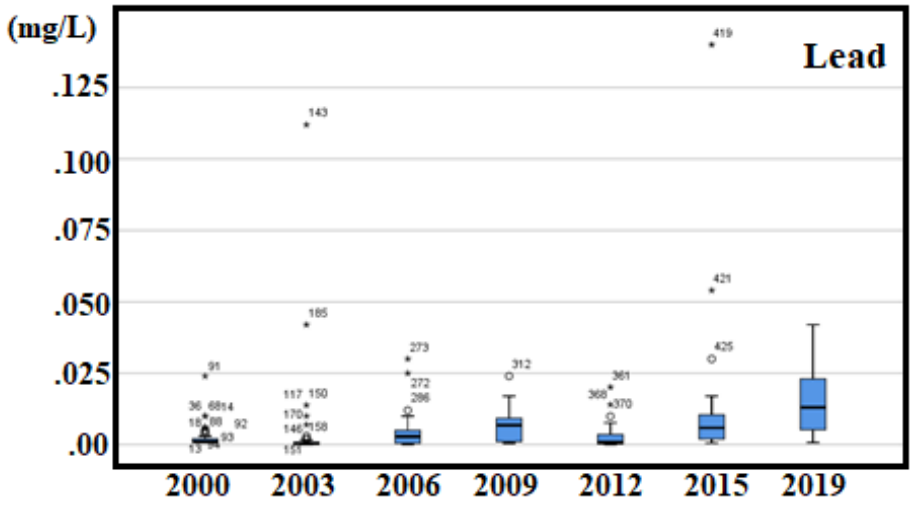

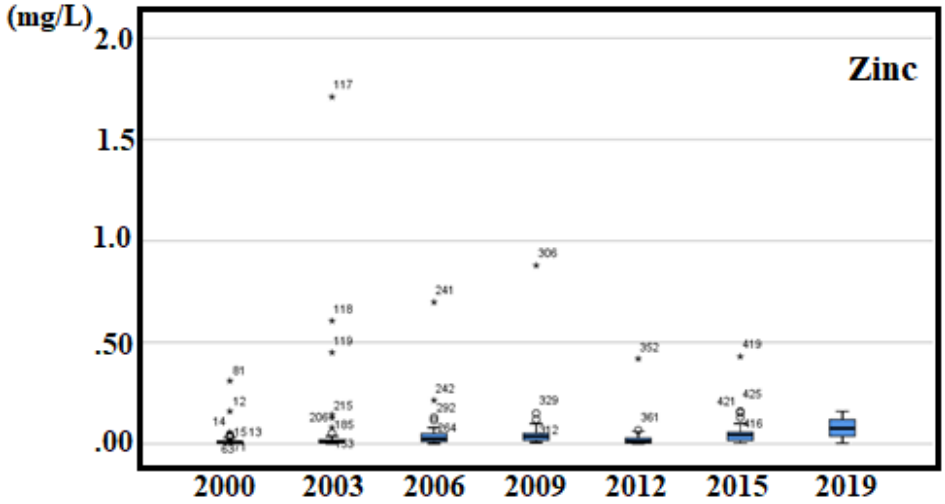

Figure 4.1 (Continued**)**

4.2 Trend in Surface Water Quality

4.2.1 Trend over Time

The results of the Mann Kendall test and the Sen's Slope estimator indicating the existence and nature of trends (increasing, decreasing, or neutral) from 2000 to 2019 in the surface water quality parameters are shown in Table 4.2. Based on a 5% significance level, the Mann Kendall test was performed to check for a statistically significant decreasing or increasing trend from 2000 to 2019. The Mann Kendall test model of interpretation was done based on the level of statistical significance often expressed as p-value, and the null and alternative hypotheses. The null hypothesis(H0) specifies the data are independent and randomly ordered (existence of no trend), and the alternative hypothesis (H1) expresses significant increasing or decreasing trend in data over time. The p-value is the level of statistical significance or the probability for the variate to be observed as a value greater than or equal to the value observed. If the p-value is lower than 0.05 based on a 5% significance level, then the alternative hypothesis is accepted and the null hypothesis rejected. And if the p-value is greater than 0.05, then the null hypothesis will be accepted.

As shown in Table 4.2, seven parameters (Fe, pH, P, Cu, Ni, Pb, and Zn) indicated increasing trends in their concentration from 2000 to 2019. The rest of the parameters have similar decreasing trends in their concentration from 2000 to 2019. Data from Table 4.2 show that statistically significant trend at 5% significance level (p-value < 0.05) of surface water quality parameters were only detected for the three parameters of Na, K (statistically significant decreasing trend detected), and Pb (statistically significant increasing trend detected).

Table 4-2 Mann Kendall trends and Sen's Slope Estimator of Parameters from 2000 to 2019

	MANN KENDHALL AT 5% SIGNIFICANCE LEVEL				SEN'S SLOPE METHOD		
Parameters	**Kendall's Tau**	**MK Statistics**	**p-value**	**Interpretation**	**Slope**	**Intercept**	**Nature of trend**
Ca	-0.62	-13	0.07	Accept H0(NSTD)	-0.202	412.68	Decreasing
Mg	-0.05	-1	1.00	Accept H0(NSTD)	-0.002	5.44	Decreasing
Na	-0.71	-15	0.04	Reject H0(STD)	-0.343	695.77	Decreasing
K	-0.71	-15	0.04	Reject H0(STD)	-0.094	192.14	Decreasing
Fe	0.24	5	0.55	Accept H0(NSTD)	0.007	-14.72	Increasing
SO4	-0.05	-1	1.00	Accept H0(NSTD)	-0.031	73.96	Decreasing
Cl	-0.24	-5	0.55	Accept H0(NSTD)	-0.068	143.52	Decreasing
NO3	-0.24	-5	0.55	Accept H0(NSTD)	-0.008	16.26	Decreasing
SiO2	-0.14	-3	0.76	Accept H0(NSTD)	-0.045	99.79	Decreasing
EC	-0.43	-9	0.23	Accept H0(NSTD)	-0.001	2.02	Decreasing
pH	0.62	13	0.07	Accept H0(NSTD)	0.011	-15.62	Increasing
P	0.33	7	0.37	Accept H0(NSTD)	0.001	-2.69	Increasing
Cu	0.52	11	0.13	Accept H0(NSTD)	0.001	-1.50	Increasing
Cr	-0.33	-7	0.37	Accept H0(NSTD)	-0.000055	0.11	Decreasing
Ni	0.24	5	0.55	Accept H0(NSTD)	0.000039	-0.08	Increasing
Mn	-0.33	-7	0.37	Accept H0(NSTD)	-0.002	4.84	Decreasing
Pb	0.81	17	0.02	Reject H0(STD)	0.001	-1.36	Increasing
Zn	0.52	11	0.13	Accept H0(NSTD)	0.002	-4.02	Increasing

NSTD: No Significant Trend Detected at 5% significance level
STD: Significant Trend Detected at 5% significance level

4.2.2 Trend over Latitude of the location of the sample sites

The nature and magnitude of trends in water quality parameters over latitude are shown in table 4.3. Given that Chattahoochee River runs approximately from north to south, the mean of the values for each parameter in each station was plotted against the latitude of the location of the sample sites to check the north to south variations and find the trend among the parameters roughly along the length of the river. It is revealed that all the parameters have similar spatial trend (increase toward the south) except for Ca, Fe, and pH that decrease toward the south and P, Cu, and Cr that maintain a constant trend over latitude.

Table 4-3 Nature and magnitude of trend in water quality parameters over the decreasing latitude of the station.

Parameters	Slope	Intercept	Nature of trend
Ca	14.865	-492.180	Increasing
Mg	-2.183	75.848	Decreasing
Na	-8.742	300.115	Decreasing
K	-1.912	67.651	Decreasing
Fe	0.000	0.125	Increasing
SO4	-15.407	529.057	Decreasing
Cl	-8.546	294.505	Decreasing
NO3	-0.841	29.042	Decreasing
SiO2	-6.960	247.316	Decreasing
EC	-0.096	3.339	Decreasing
pH	0.335	-4.406	Increasing
P	0.000	0.095	Neutral
Cu	0.000	0.002	Neutral
Cr	0.000	0.001	Neutral
Ni	-0.002	0.078	Decreasing
Mn	-0.170	5.789	Decreasing
Pb	-0.00025	0.009	Decreasing
Zn	-0.021	0.718	Decreasing

4.3 Principal factor governing geochemical processes

Table 4.4 presents the total variance explained from the PCA i.e., the eigenvalues, the cumulative eigenvalue, the percentage of variance, and the associated cumulative percentage of variance. The PCA was performed using the mean from 2000 to 2019 of selected water quality parameters to identify parameters influencing geochemical processes in the study area. The PCA results reveal five significant PCs explaining 84.228 % of the total variance.

Table 4-4 Total variance explained

Total Variance Explained									
Comp	Initial Eigenvalues			Extraction Sums of Squared Loadings			Rotation Sums of Squared Loadings		
	Total	% of Variance	Cumulative %	Total	% of Variance	Cumulative %	Total	% of Variance	Cumulative %
1	7.559	41.994	41.994	7.559	41.994	41.994	6.369	35.385	35.385
2	2.846	15.811	57.804	2.846	15.811	57.804	3.398	18.876	54.261
3	2.055	11.419	69.223	2.055	11.419	69.223	2.173	12.070	66.331
4	1.773	9.849	79.072	1.773	9.849	79.072	2.038	11.325	77.656
5	0.928	5.155	84.228	0.928	5.155	84.228	1.183	6.572	84.228
6	0.812	4.512	88.739						
7	0.710	3.945	92.684						
8	0.342	1.902	94.587						
9	0.328	1.820	96.407						
10	0.193	1.075	97.481						
11	0.153	0.851	98.332						
12	0.101	0.560	98.892						
13	0.078	0.436	99.328						
14	0.050	0.278	99.606						
15	0.031	0.171	99.778						
16	0.026	0.145	99.923						
17	0.010	0.056	99.979						
18	0.004	0.021	100.000						

Table 4.5 presents loading of rotated factor matrix for the five PCs using the varimax method (Forina et al., 2005). Since each factor accounts for as much of the remaining variance as possible, it is evident from Table 4.5 that the water quality parameters are generally more correlated with the first component. To identify the parameters influencing geochemical processes in the study area for surface water, the PC loadings were classified (Table 4.5) based on the criteria defined by Liu et al. (2003). According to the criteria, the PC loading were sorted as weak, moderate, and strong, corresponding respectively to the absolute values of 0.30-0.5, 0.5-0.75, and more than 0.75.

Table 4-5 Principal component loadings for varimax rotated factor matrix explaining 84.228% of the total variances

	COMPONENT				
	1	2	3	4	5
Ca	0.731	0.518	0.305	0.233	0.063
Mg	0.906	0.213	0.216	0.123	0.162
Na	0.982	0.020	0.126	-0.029	-0.044
K	0.948	0.176	-0.010	0.101	-0.042
Fe	0.063	0.657	-0.604	0.054	0.172
SO4	0.043	0.883	0.243	-0.129	0.082
Cl	0.902	0.249	0.172	-0.044	-0.045
NO3	0.256	0.594	0.085	0.228	-0.107
SiO2	0.351	0.229	0.745	-0.005	0.286
EC	0.932	0.190	0.113	0.094	0.123
pH	0.301	-0.005	0.772	-0.073	-0.027
P	0.129	0.052	-0.512	-0.394	-0.233
Cu	0.002	0.126	-0.144	0.895	-0.181
Cr	0.050	0.061	0.136	-0.070	0.942
Ni	0.500	0.721	-0.269	0.003	0.156
Mn	0.948	-0.062	-0.011	-0.142	-0.014
Pb	0.101	0.095	0.126	0.928	0.061
Zn	0.075	0.885	-0.058	0.165	-0.012

Table 4-6 Parameters grouping based on the nature of the principal component loadings

	NATURE OF LOADING		
	STRONG	MODERATE	WEAK
Component I	Mg, Na, K, Cl, EC, Mn	Ca, Ni	SiO2, pH,
Component II	SO4, Zn	Ca, Fe, NO3, Ni	-
Component III	pH	Fe, SiO2, P	Ca
Component IV	Cu, Pb	-	P
Component V	Cr	-	-

Table 4-7 Matrix of correlation coefficients for hydrochemical data in the study area

	Ca	Mg	Na	K	Fe	SO4	Cl	NO3	SiO2	EC	pH	P	Cu	Cr	Ni	Mn	Pb	Zn
Ca	1	0.889	0.75	0.812	0.222	0.569	0.811	0.56	0.624	0.845	0.427	0.071	0.229	0.167	0.622	0.608	0.396	0.508
Mg		1	0.9	0.883	0.081	0.288	0.86	0.408	0.568	0.953	0.38	0.087	0.059	0.222	0.547	0.85	0.259	0.277
Na			1	0.919	0.006	0.102	0.938	0.252	0.422	0.931	0.4	0.072	0.018	0.03	0.462	0.931	0.081	0.089
K				1	0.187	0.164	0.875	0.416	0.358	0.887	0.284	0.1	0.123	0.017	0.612	0.867	0.19	0.214
Fe					1	0.402	0.13	0.221	-0.21	0.12	-0.33	0.252	0.166	0.063	0.721	0.003	0.085	0.613
SO4						1	0.298	0.469	0.363	0.273	0.192	0.024	0.013	0.212	0.54	6.3e-5	0.001	0.703
Cl							1	0.368	0.497	0.894	0.436	0.089	0.013	0.057	0.592	0.789	0.086	0.246
NO3								1	0.27	0.352	-0.08	0.094	0.267	0.017	0.468	0.165	0.181	0.429
SiO2									1	0.468	0.591	0.282	0.156	0.368	0.189	0.266	0.21	0.159
EC										1	0.317	0.011	0.061	0.174	0.564	0.86	0.224	0.26
pH											1	0.214	0.101	0.133	0.017	0.265	0.107	0.013
P												1	0.096	0.125	0.092	0.078	0.316	0.031
Cu													1	-0.17	0.073	0.162	0.779	0.225
Cr														1	0.132	0.015	0.002	0.005
Ni															1	0.441	0.098	0.709
Mn																1	0.058	0.056
Pb																	1	0.27
Zn																		1

4.4 Lineament and density maps of the study area

Figure 4.2 presents the lineament map and the lineament density map of the Atlanta metropolitan along with the rose diagrams (lineament number, length, and orientation). The lineament density represents magnitude-per-unit area from lineament features that fall within a radius around each cell. They show the maximum intersection points of the lineaments and their orientations, which gives a sense of fractured rock permeability that conducts ions in the surface water to contaminate groundwater.

Figure 4.3 shows the land use and land cover (LULC) map from Landsat 8 image using the unsupervised classification method. The classification system divides the land use types into five types: Urban, Forest, Grassland, Water, and Exposed and Cultivated land (Figure 4.3).

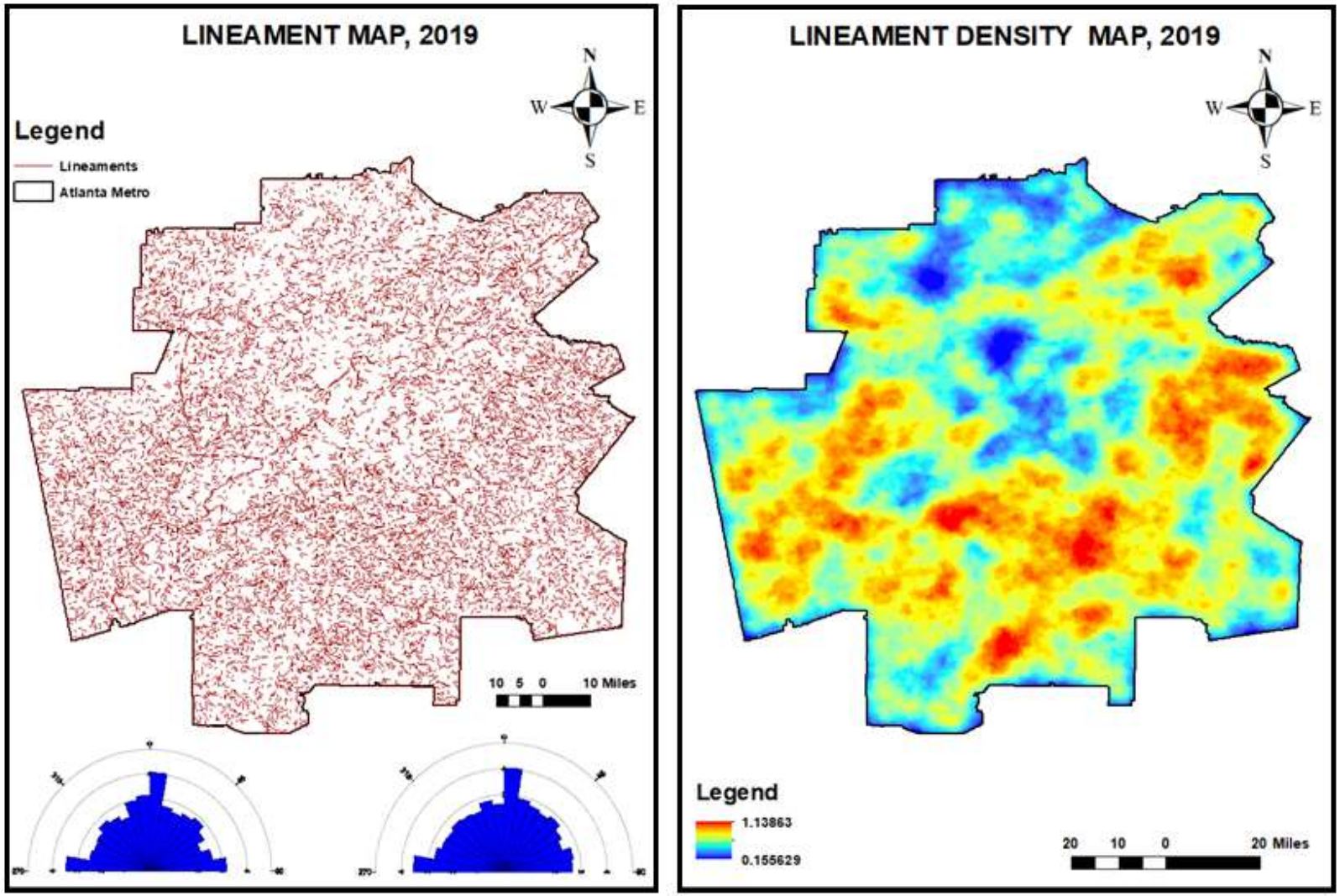

Figure 4-2 Lineament map and lineament density map (magnitude-per-unit area) of Atlanta metropolitan

4.5 Land Use and Land Cover (LULC) Analysis

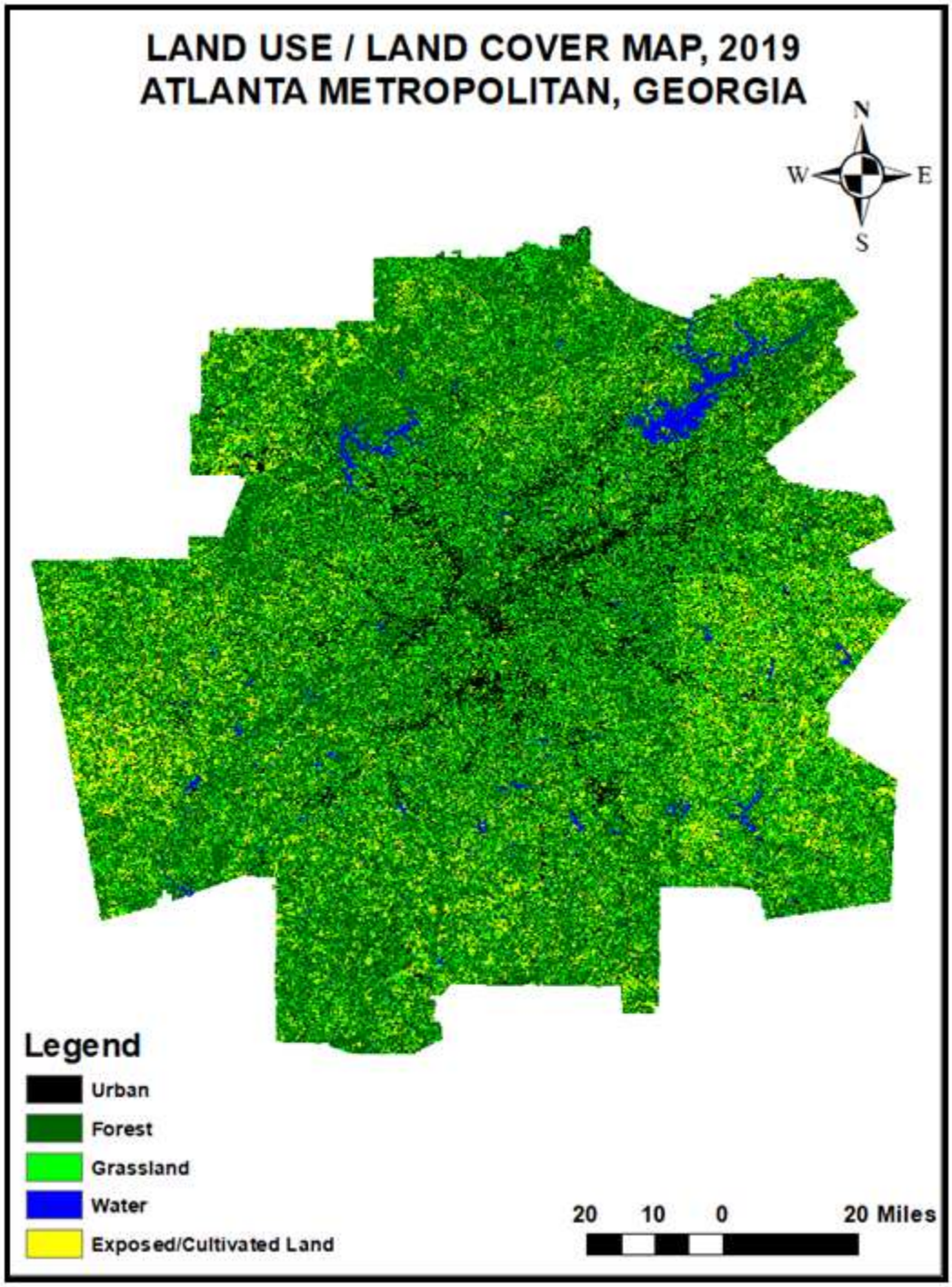

Figure 4-3 LULC Map of Atlanta Metropolitan

4.6 Multi-distance spatial cluster analysis of contaminant sources

Figure 4.4 shows the distribution of Toxic Release Inventory (TRI) facilities or contaminant sources across the Atlanta metropolitan from 2000 to 2019. Such contaminant sources are typically larger facilities involved in manufacturing, metal mining, electric power generation, chemical manufacturing, and hazardous waste treatment. As shown in Figure 4.4, the number of pollution sources increased from 2000 to 2019. Fulton, Dekalb, Cobb, and Gwinnett counties contain much more facilities than other counties.

The results from Ripley's K-function analysis (Figure 4.5) show a significant clustering of sources of contaminants in 2000, 2003, 2006, 2009, 2012, 2015, and 2019. The observed K values are larger than the expected K values according to the K-function graphs from 2000 to 2019. Hence, the distribution is more clustered than a random distribution (Figure 4.4).

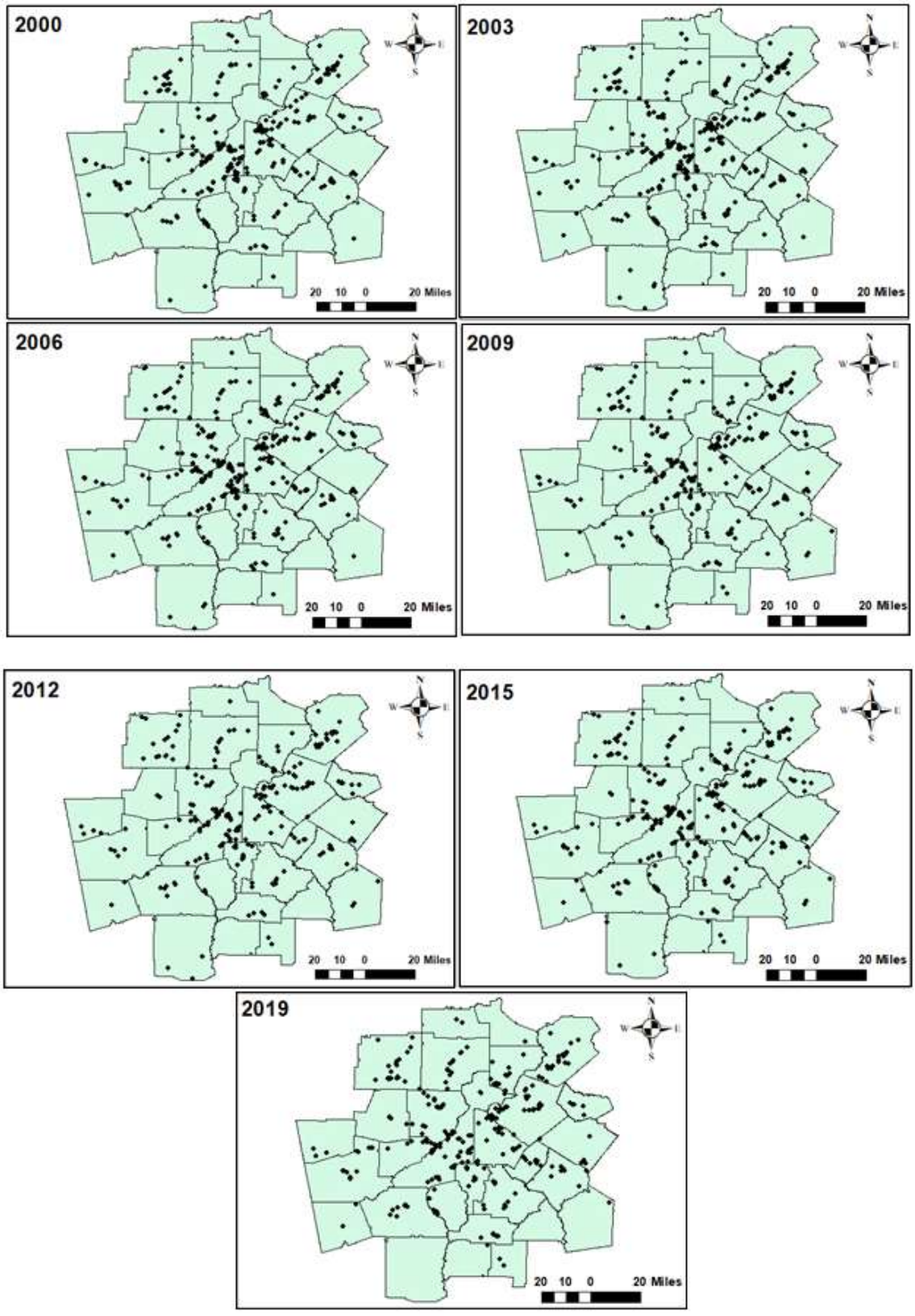

Figure 4-4 Distribution of TRI facilities across Atlanta metropolitan from 2000 to 2019

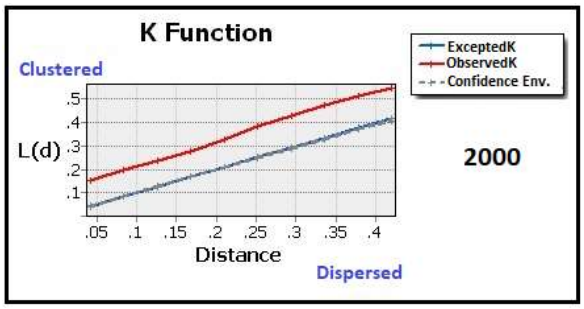

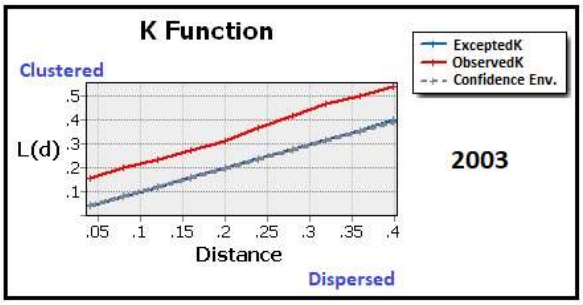

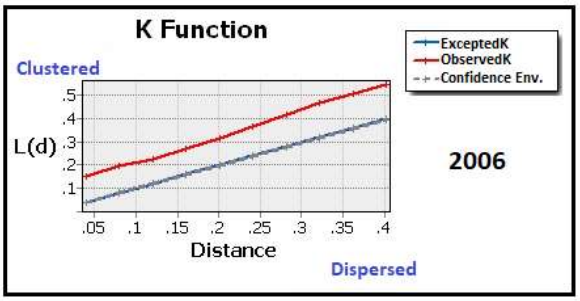

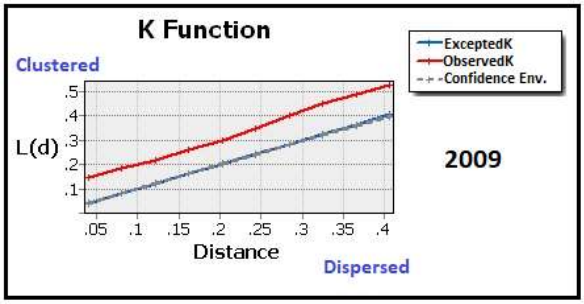

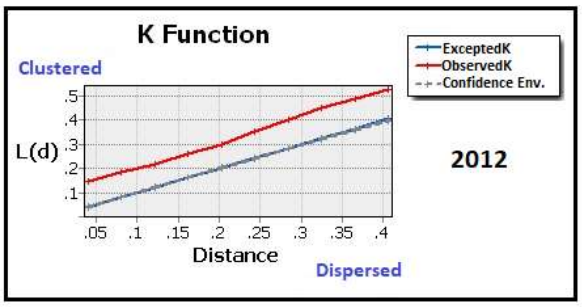

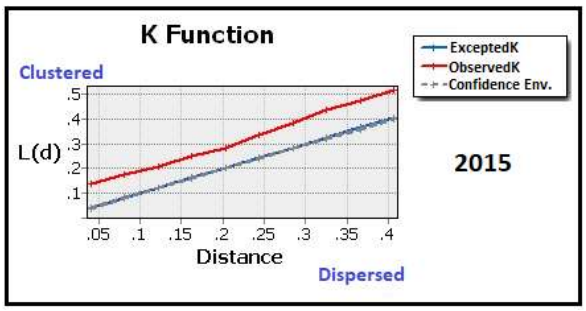

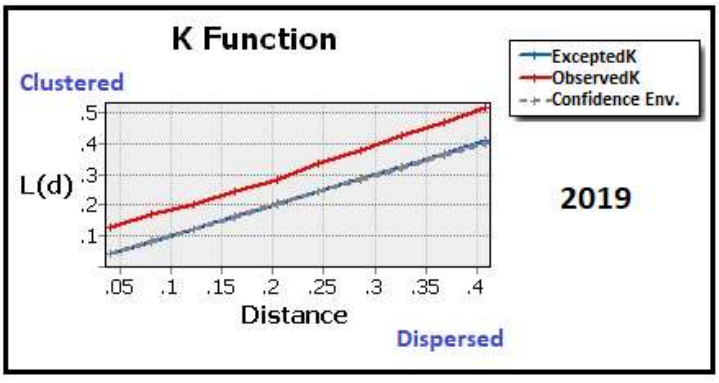

Figure 4-5 K Function graphs of TRI from 2000 to 2019 in Atlanta metropolitan.

4.7 Spatio-temporal variations of quantity of chemicals released in the study area

Figures 4.6, 4.7, 4.8, and 4.9 present the distribution of the total quantity of chemicals released across the Atlanta metropolitan from 2000 to 2019. This includes the quantity of chemicals released on-site as surface water discharges, to on-site landfills, into surface impoundments, injected on-site at the facility to underground injection wells, disposed of through on-site land treatment/application farming, and chemical that was transferred to a POTW (publicly owned treatment works). The type of chemicals covered by the TRI Program and included in this study are those that cause cancer or other chronic human health effects, significant adverse acute human health effects, and significant adverse environmental effects. The list of the type of chemicals used in this study is omitted here to keep the thesis within the required length, and can be found in TRI Chemical List.

As shown in the Figures from 2000 to 2019, the contaminated area has been spreading from the central metropolitan area. Fulton, Dekalb, Coweta, and Cobb counties have received the highest amount of toxics release than other counties from 2000 to 2012. In 2015, the highest amount of chemicals released were found in Clayton, Heard, Walton, Barrow, Gwinnett, Bartow, and Forsyth counties. Finally, in 2019, the contaminated area became wider affecting different counties along with the central metropolitan area

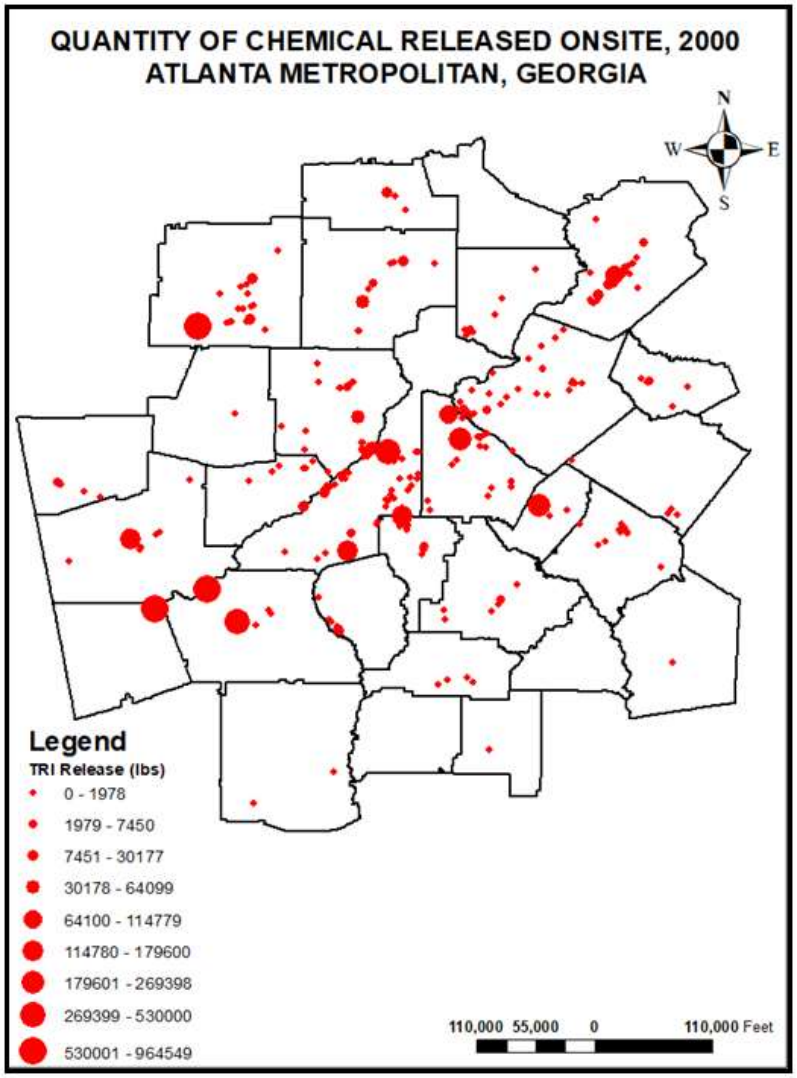

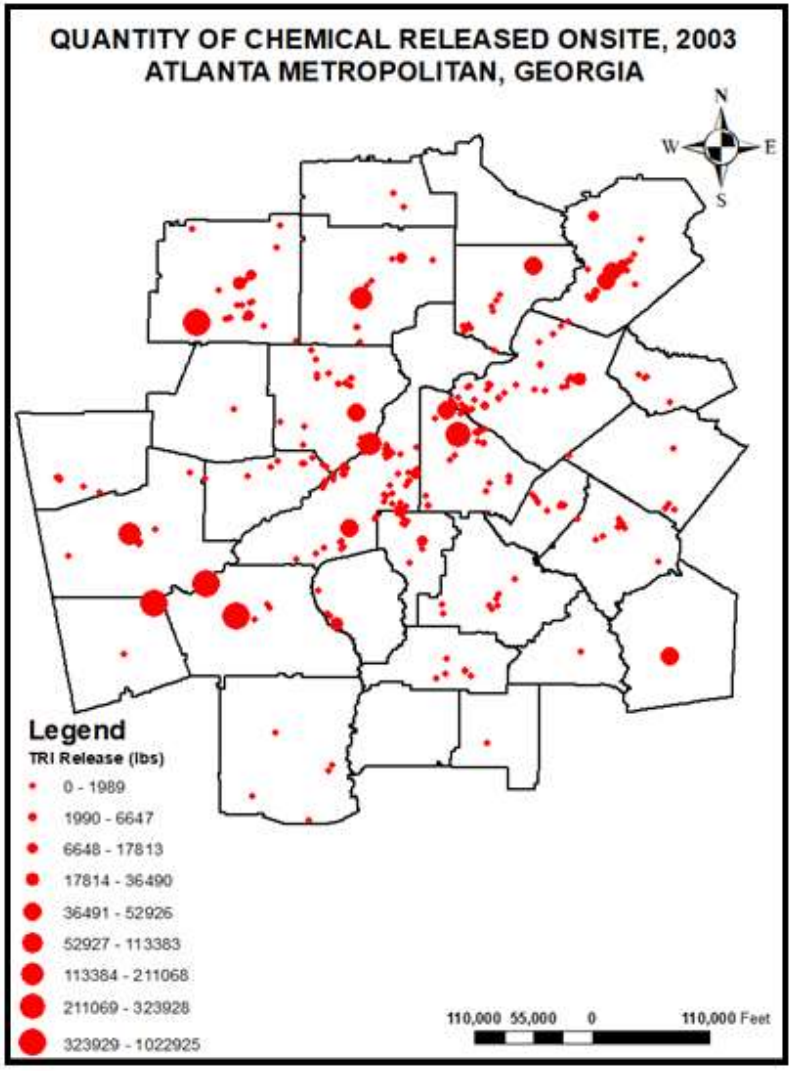

Figure 4-6 Toxic Release Inventory (TRI) in 2000 and 2003

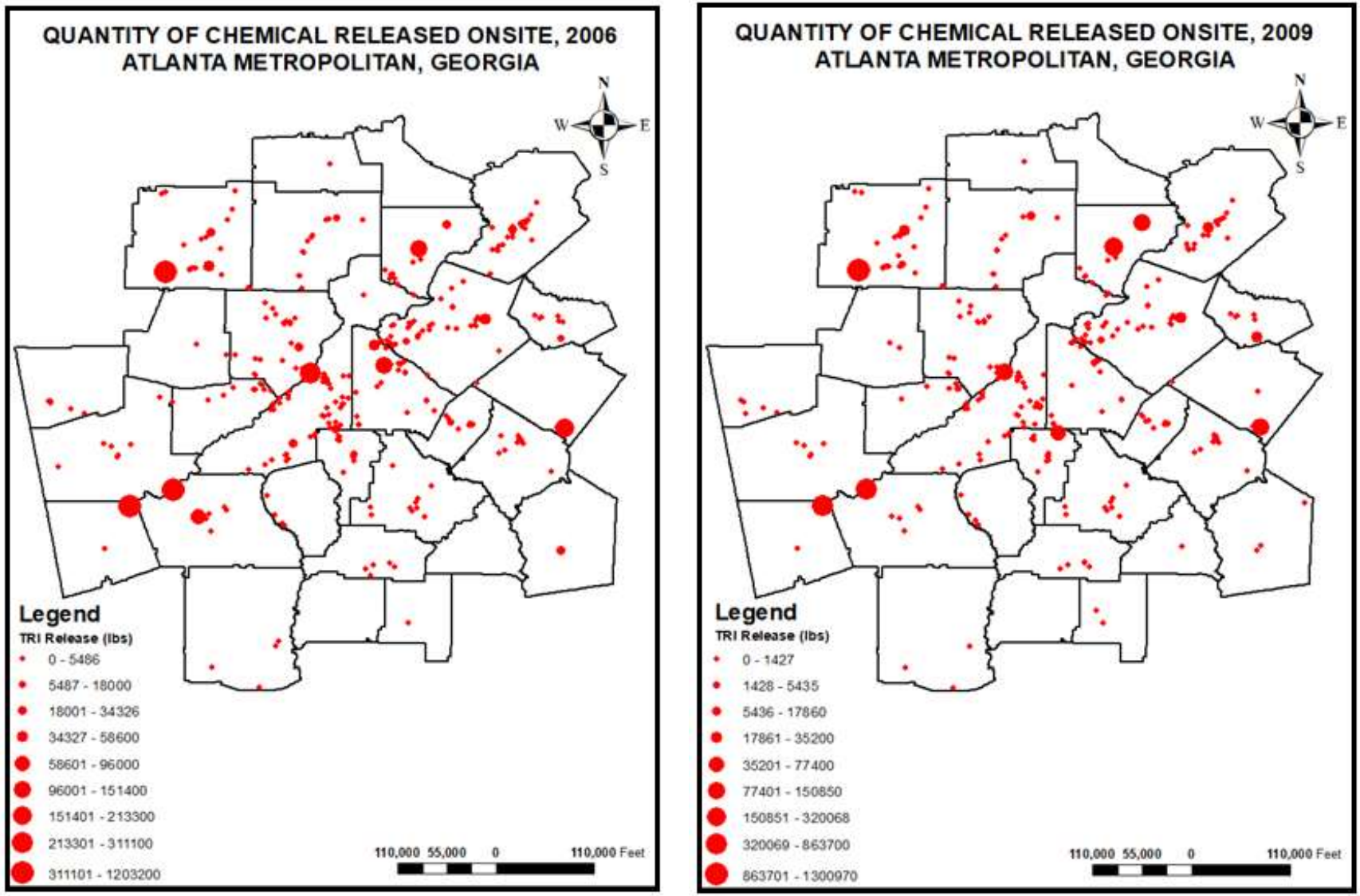

Figure 4-7 Toxic Release Inventory (TRI) in 2006 and 2009

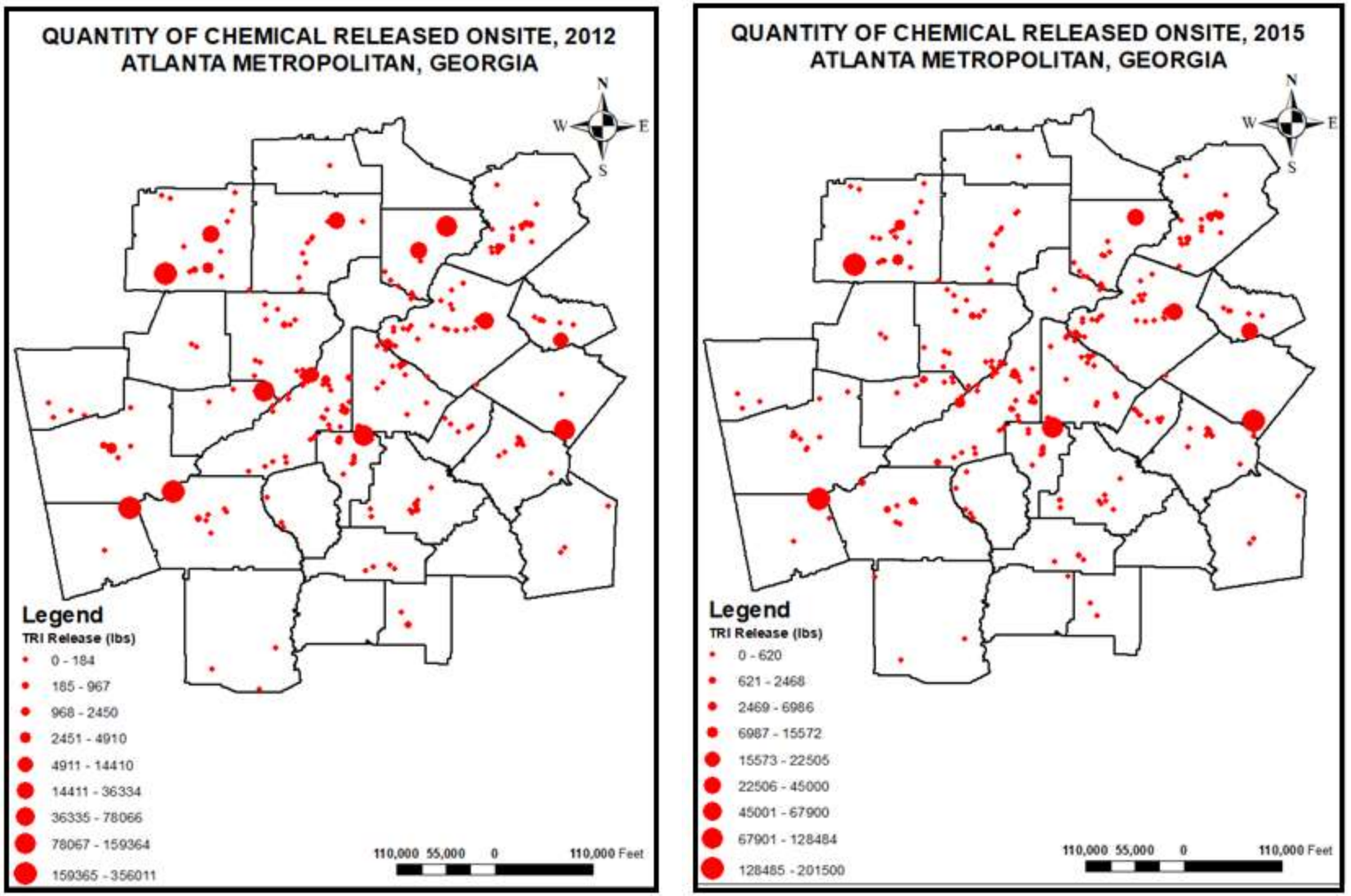

Figure 4-8 Toxic Release Inventory (TRI) in 2012 and 2015

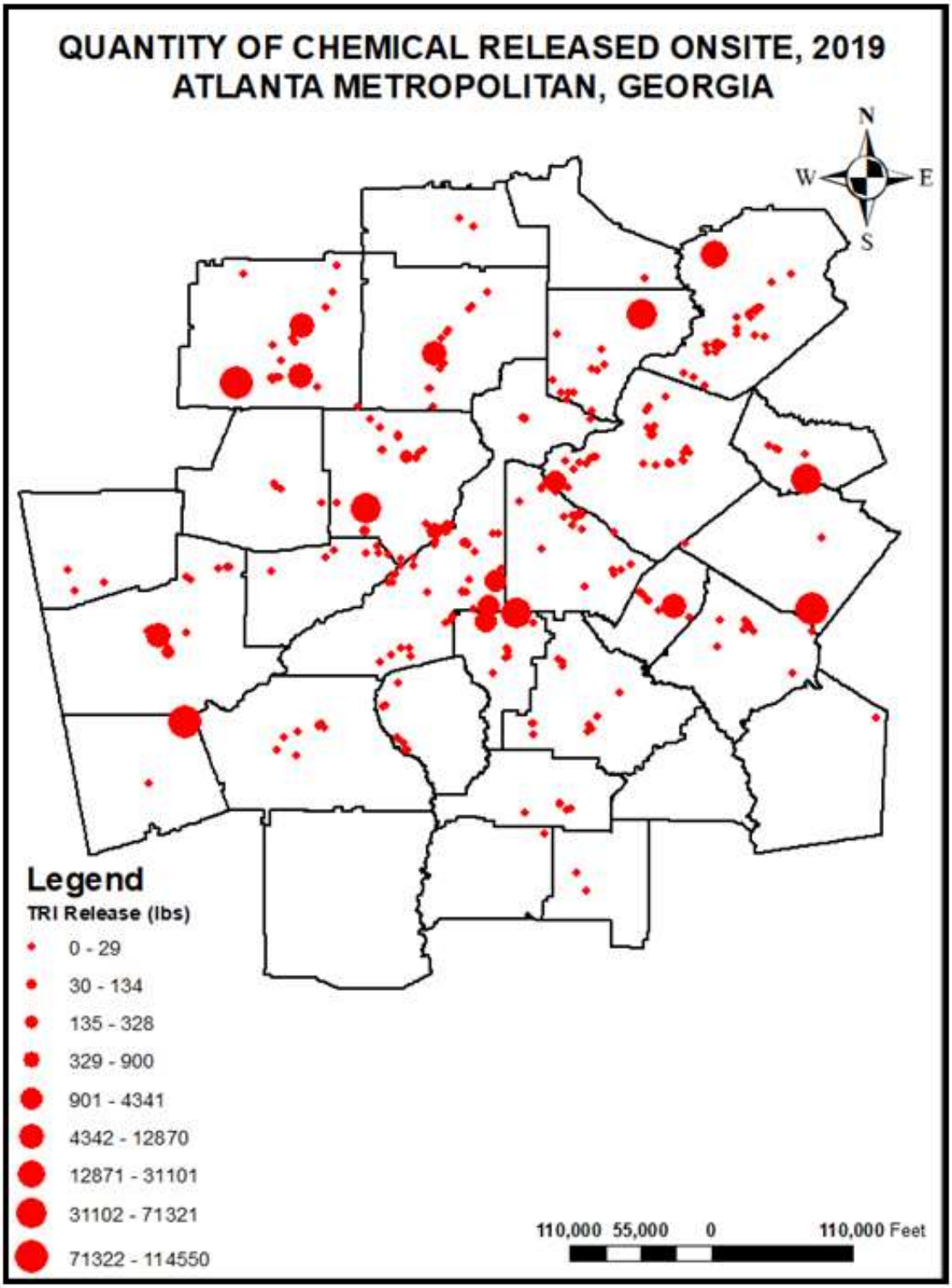

Figure 4-9 Toxic Release Inventory (TRI) in 2019 *j*

4.8 Environmental justice analysis

4.8.1 Distribution of TRI facilities and onsite release by income

Spatial distribution of TRI facilities and the total quantity of chemicals released across the Atlanta metropolitan were correlated with income, race, age, and sex using county-level census data in 2019.

Figures 4.10 and Figure 4.11 present respectively the spatial distribution of the TRI facilities and the total quantity of chemicals released by median household income in 2019. As shown in Figure 4.10, high median household income counties concentrate much more on TRI facilities. These high median household income counties are located in the center of the metropolitan area (Gwinnett, Fulton, Cobb, Cherokee, Forsyth, Paulding, Coweta, Fayette, and Henry). Counties with low to intermediate median household income seem to concentrate on fewer or no TRI facilities. However, when compared to the quantity of chemicals released in 2019 (Figure 4.11), counties with low to intermediate median household income are more exposed to contaminants, as the highest quantity of chemicals released is recorded in there. This demonstrates disproportionate exposures to environmental hazards based on median household income regarding TRI facilities and hazardous chemicals.

.

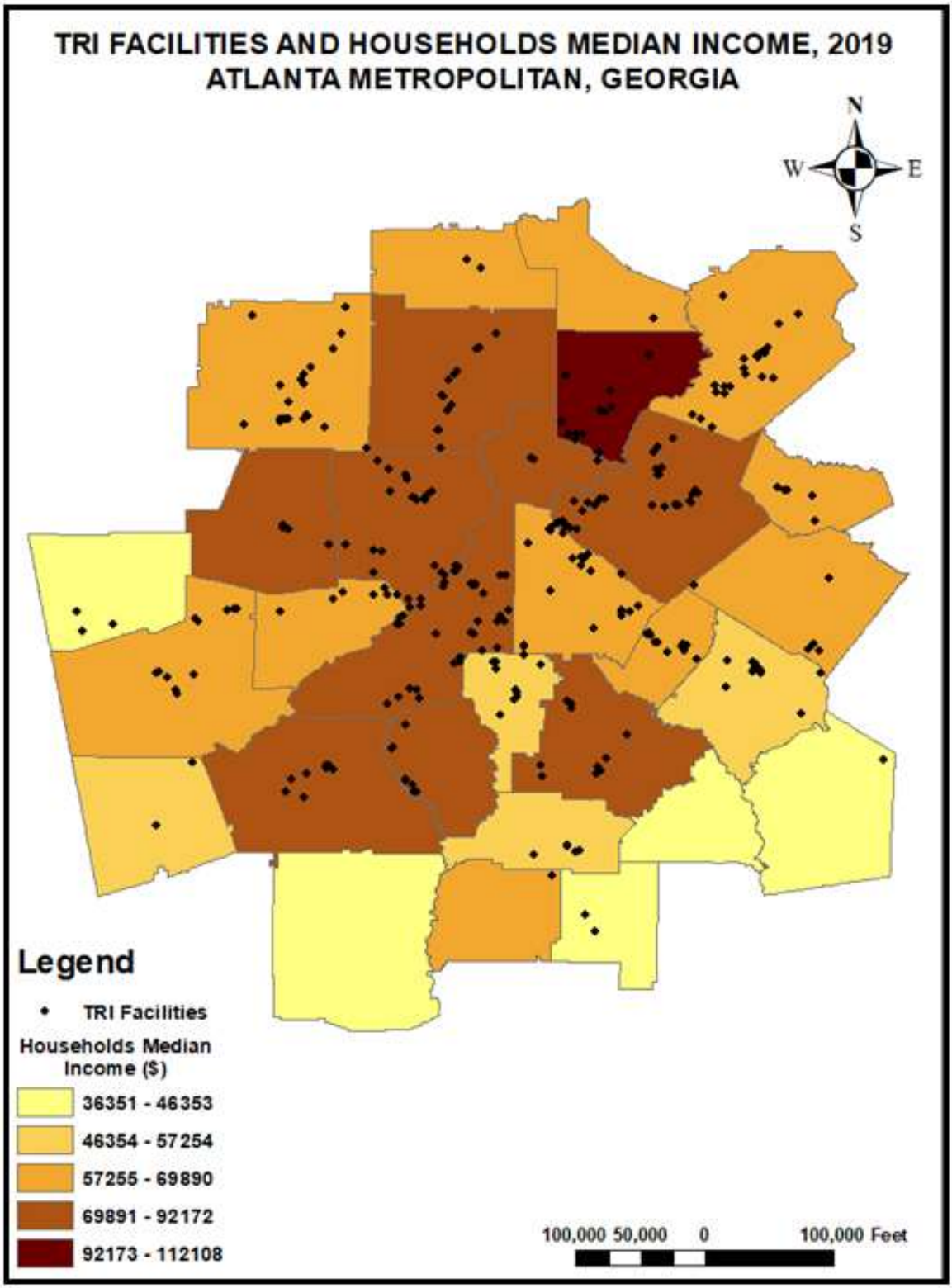

Figure 4-10 TRI Facilities distribution and households median income in 2019

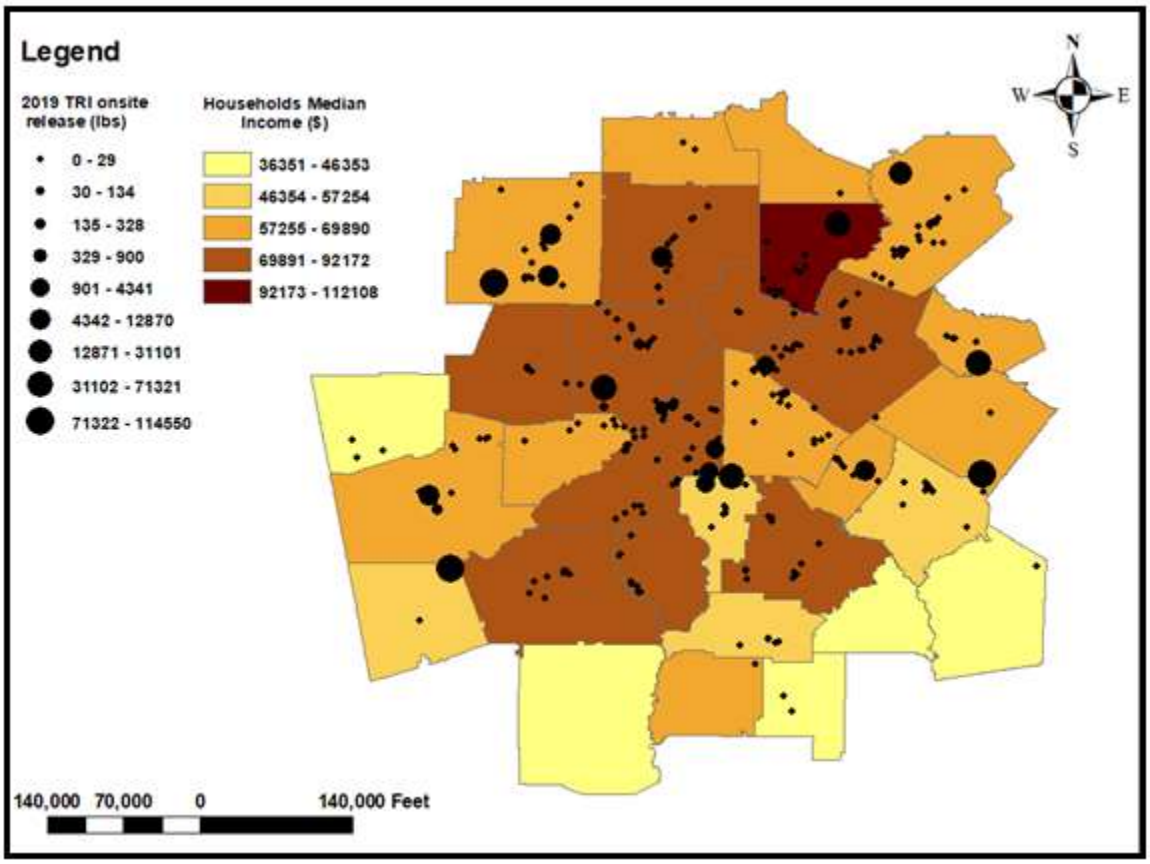

Figure 4-11 TRI Onsite Release and Households Median Income in 2019

4.8.2 Distribution of TRI facilities and onsite release by race

Figures 4.12 and Figure 4.13 show the spatial distribution of TRI facilities by race (fractions of black and white population, and the ratio of black over white). Such figures reveal a concentration of high fraction of black population in the center of the metro area, where a high number of TRI facilities is present compared to counties with high fraction of white population.

Figure 4.14 and Figure 4.15 present the spatial distribution of the total quantity of chemicals released by race (fractions of black and white population, and the ratio of black over white). As shown in the figures, the highest quantity of chemicals released is recorded in counties with a low ratio of black over white. However, counties with a high ratio of black over white are more exposed to TRI facilities. But, some northern counties with high fraction of white population (Bartow, Cherokee, and Hall) present high TRI facilities and high quantity of chemicals released. Moreover, in these counties the distribution of the TRI facilities seems to be linear. This shows disproportionate exposures to environmental hazards based on race.

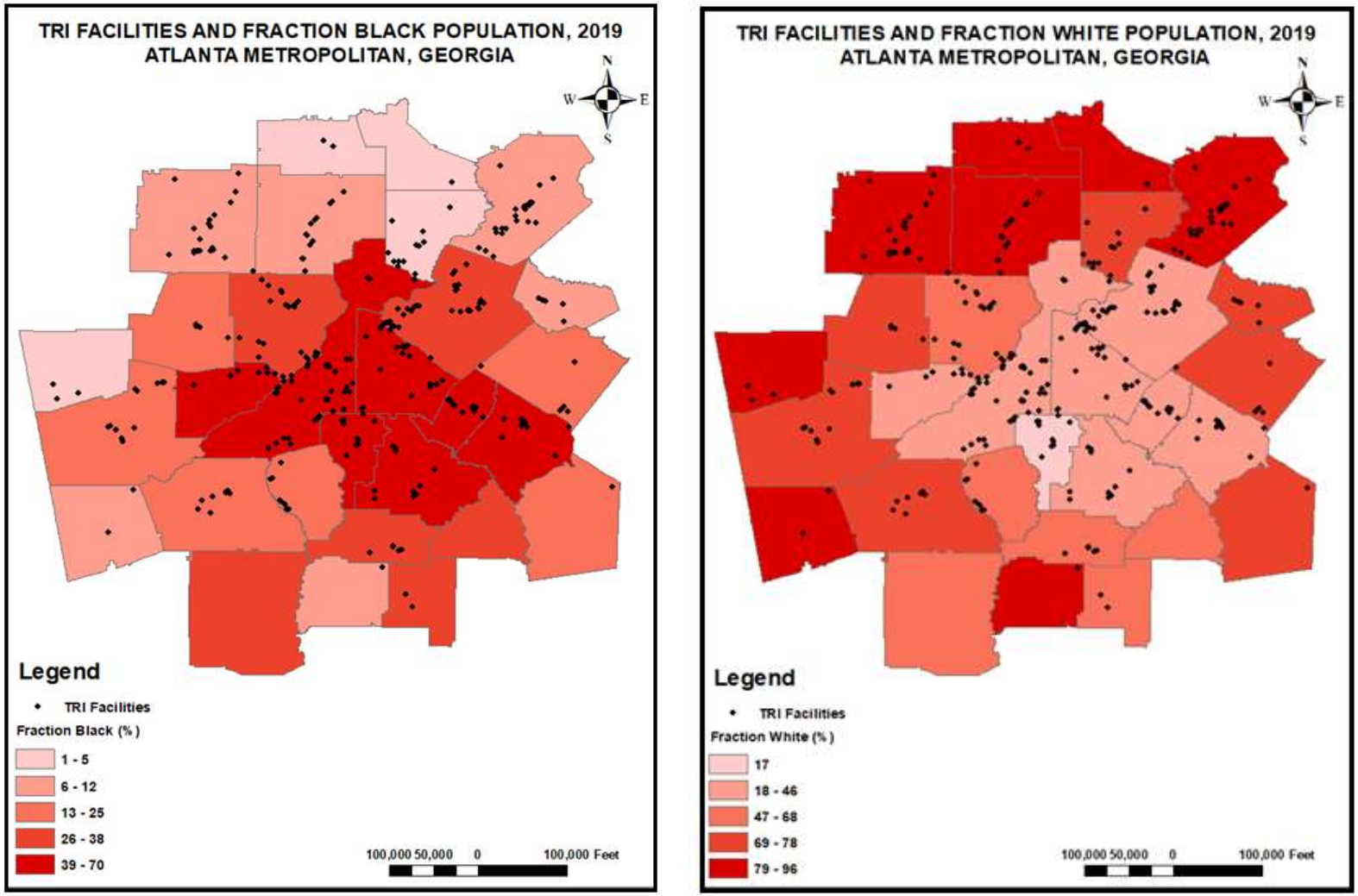

Figure 4-12 TRI Facilities distribution and black and white population in 2019

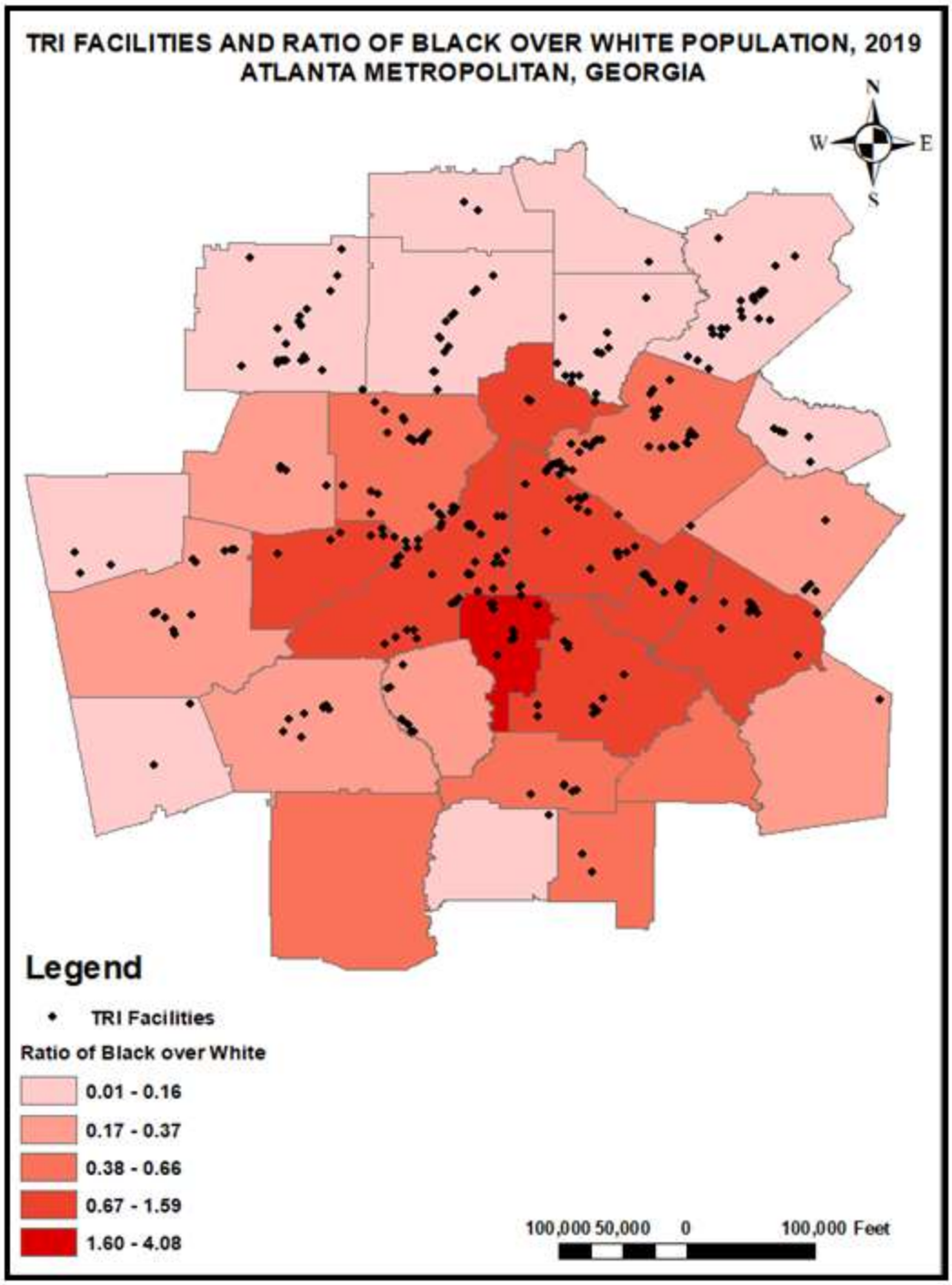

Figure 4-13 TRI Facilities distribution and ratio of black over white population in 2019

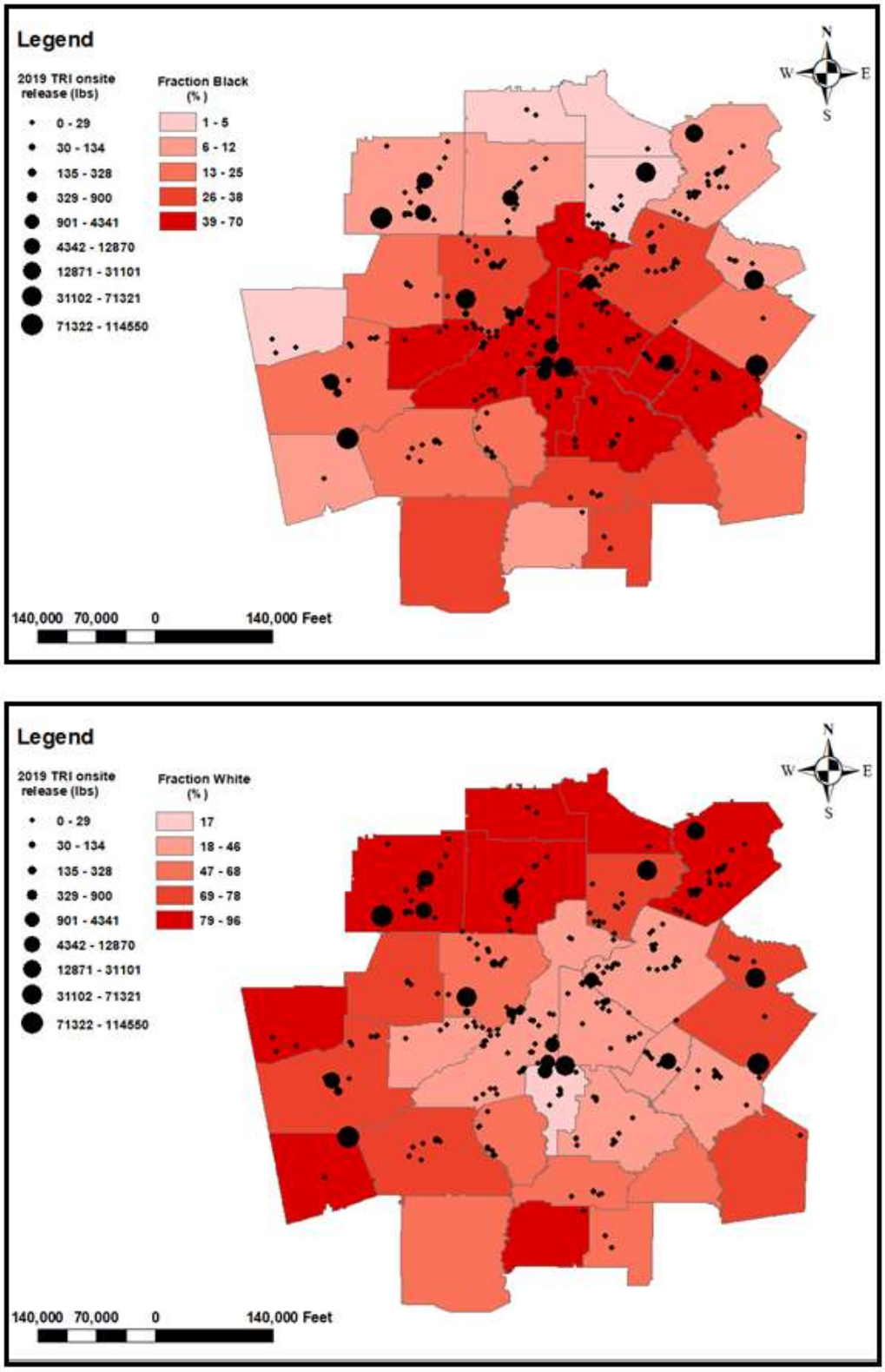

Figure 4-14 TRI onsite release and black and white population in 2019

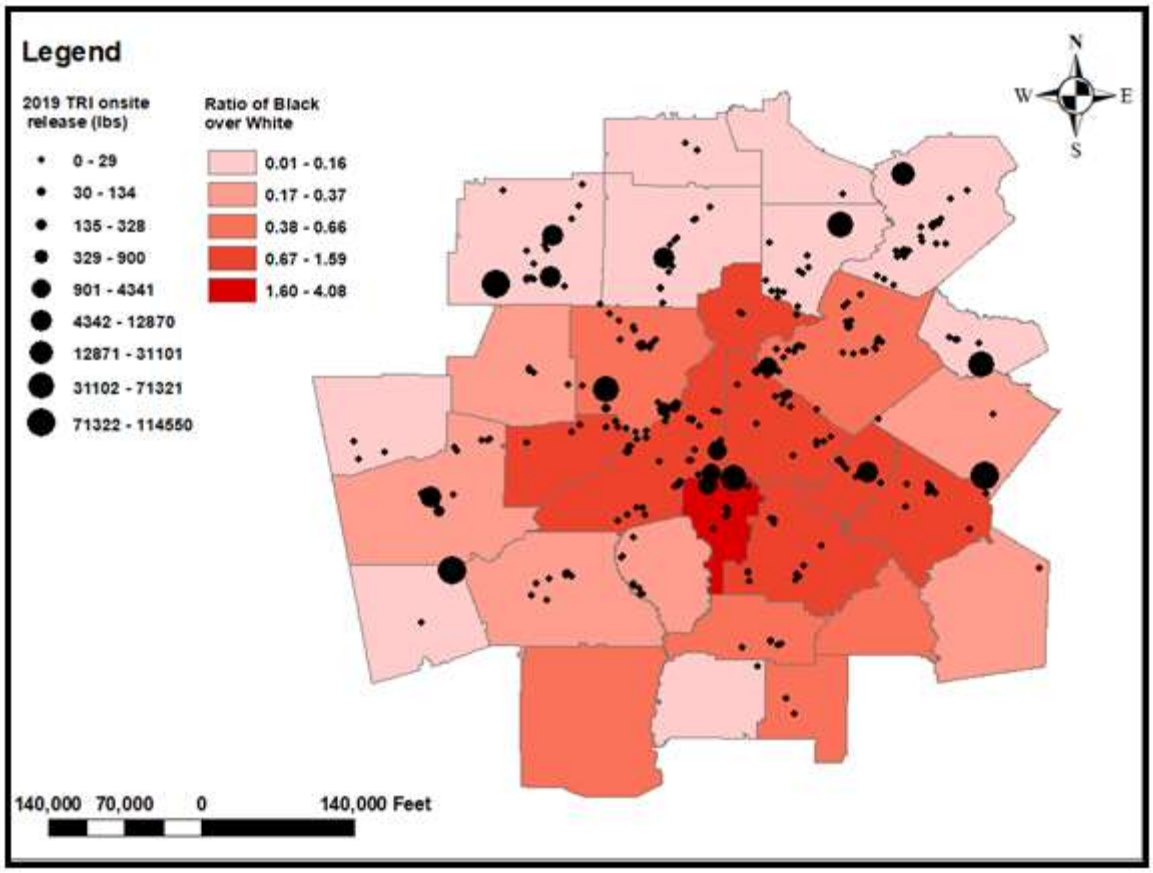

Figure 4-15 TRI onsite release and ratio of black over white population in 2019

4.8.3 Distribution of TRI facilities and onsite release by age

Figures 4.16 and Figure 4.17 present respectively spatial distribution of TRI facilities and the total quantity of chemicals released by age in 2019. The human age is classified into four categories as Child (0-12 years), Adolescence (13-18 years), Adult (19-59 years), and Senior Adult (60 years and above). As shown in Figure 4.16 and Figure 4.17, the youngest population (median age up to 39) are more exposed to TRI facilities and chemical hazards. Counties with a median age greater than 39 concentrate approximately no TRI facilities and did not record any chemical hazards released. These counties with no chemical hazards record in 2019, located at the edges of the metro area, are Pickens, Dawson, Jasper Pike, Spalding, Meriwether, Coweta, Heard, and Haralson counties. Therefore, there is no balanced exposure to environmental hazards and the principles of environmental justice are not applied to the Atlanta metro area based on age.

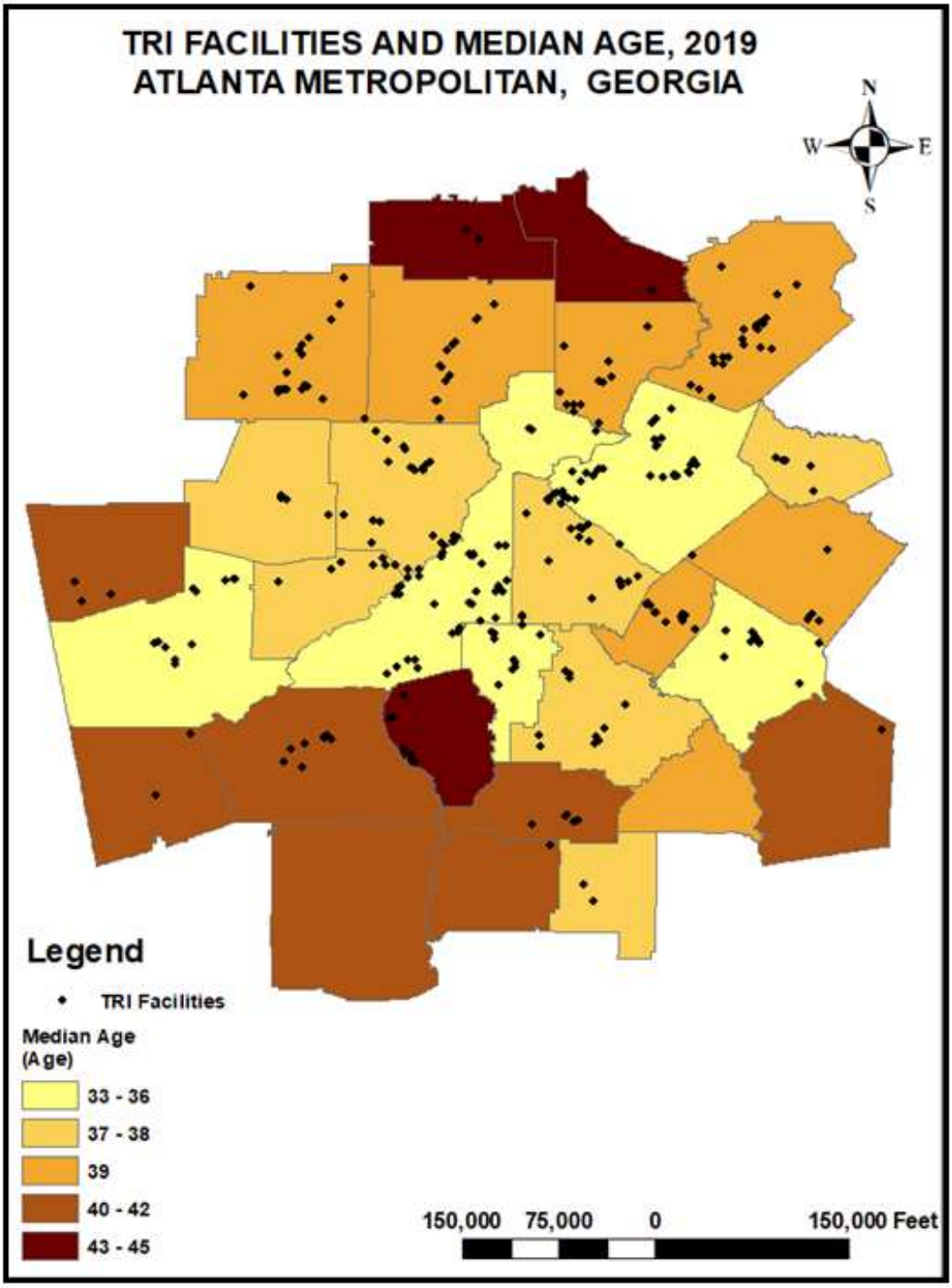

Figure 4-16 TRI facilities distribution and median age in 2019

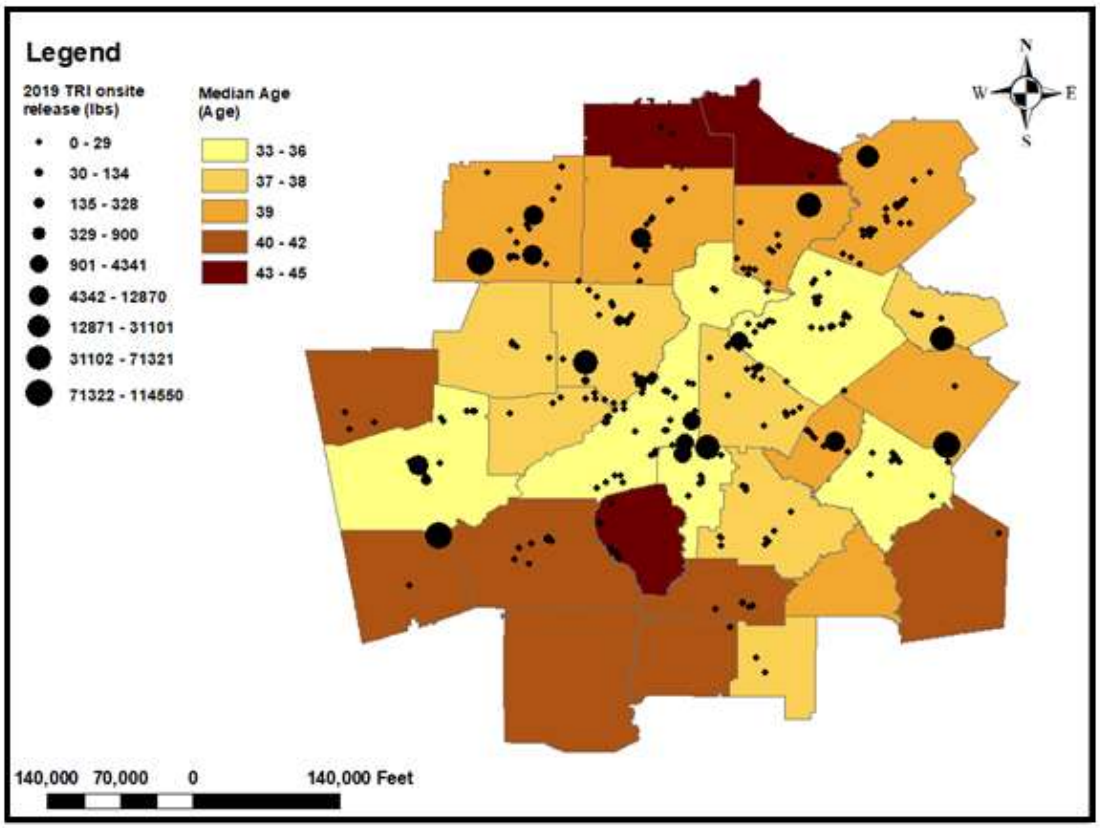

Figure 4-17 TRI onsite release and median age in 2019

4.8.4 Distribution of TRI facilities and onsite release by sex

Figures 4.18 and Figure 4.19 present respectively spatial distribution of TRI facilities and the total quantity of chemicals released by sex in 2019. As shown in Figure 4.18 and Figure 4.19, females are more exposed to TRI facilities and chemicals hazards, except for 3 counties where equal exposure to chemicals released is noticed (Barrow, Hall, and Forsyth counties). Some southern counties with high fractions of females (Coweta, Fayette, Henry, Newton, Jasper, Lamar, Pike, Meriweather, Coweta) have no chemicals released and low to no TRI facilities in 2019. However, Butts county where there are more men than female did not record any TRI facilities or chemicals released. Finally, Northwestern and central counties with highest fractions of females concentrate most of the chemicals released. This also illustrates the existence of disproportionate exposures to environmental hazards based on sex, and therefore no application of environmental justice principles to the area.

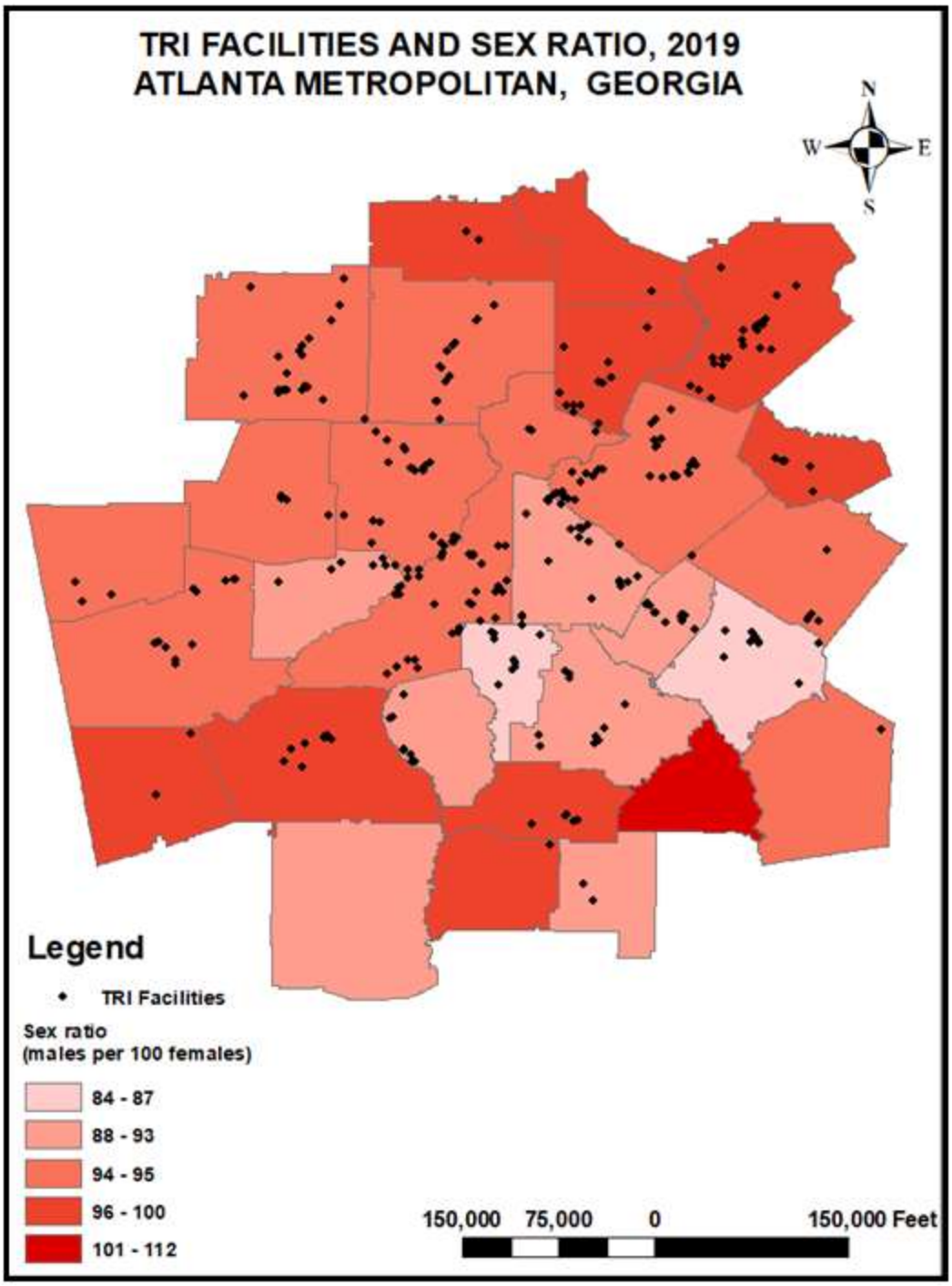

Figure 4-18 TRI Facilities distribution and sex ratio (males per 100 females) in 2019

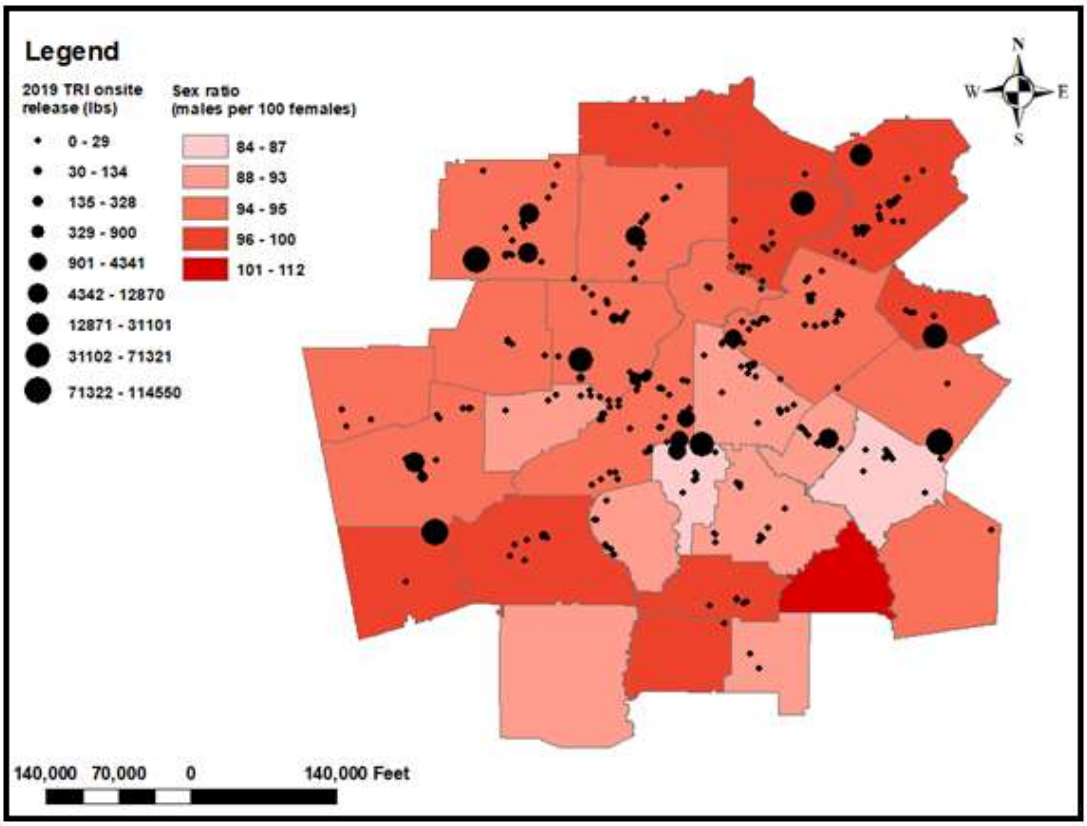

Figure 4-19 TRI Onsite Release and Sex Ratio (Males per 100 Females) in 2019

5 DISCUSSIONS

5.1 Spatio-Temporal Variations and Trend Analyses

This study found significant spatial and temporal variations in the water quality parameters across the Atlanta metropolitan area around the Chattahoochee River from 2000 to 2019. Parameters such as Ca, Mg, K, SO_2, Fe, SiO_2, NO_3, and Cl present large spatio-temporal variations compared to other parameters (a relatively large length of boxes and whiskers). Nickel and zinc present the least spatio-temporal variations with relatively small boxes and whiskers length (Fig 4.1). Box and whisker plots of Ca, Mg, K, Fe, Cl, NO3, SiO2, EC, and P reveal an important observation in 2000, 2003, and 2006. These parameters present the highest concentration in three years, 2000, 2003, and 2006, that correlates with contaminant data (quantity of chemicals released onsite). In those years, a significant amount of contaminant was received in the study area (Figure 4.6; Figure 4.7). This finding reveals that contaminant sources have control over water quality in the study area. This control of contaminant sources over water quality found in this study is concurrent with findings from Machiwal and Jha (2015) which revealed control of water contamination by contaminant sources, the geology of the study area, and anthropogenic processes. Furthermore, the significant spatial and temporal variations in the water quality parameters from 2000 to 2019 found in this study are also consistent with Jabbar and Grote's findings in 2019. The results of these authors' work indicate a significant spatio-temporal variability of physical, chemical, and biological characteristics of all small watersheds in the Lower Grand River watershed in north-central Missouri and south-central Iowa, and a negative impact of agricultural activities in many Midwestern streams and lakes.

As far as trend analysis, the Mann-Kendall test indicated the existence of increasing and decreasing trends in parameter concentration from 2000 to 2019 (Table 4.2). Thus, seven parameters such as

Fe, pH, P, Cu, Ni, Pb, and Zn indicated increasing trends in their concentration from 2000 to 2019 compared to the other parameters. However, only three parameters revealed a statistically significant trend at 5% significance level (p-value < 0.05) from 2000 to 2019. These parameters are Na, K (statistically significant decreasing trend detected), and Pb (statistically significant increasing trend detected).

This study also found north to south variations in the concentration of water quality parameters i.e., the existence of trends over the latitude of the location of the sample sites.

It is seen from Table 4.3 that parameters presenting an increasing/positive trend toward the southern direction are higher than those indicating decreasing or neutral trends. Almost all the parameters have a similar trend (increase toward the south) except for Ca, Fe, and pH (indicating decreasing trends toward the south), and P, Cu, Cr (constant trends over latitude). This indicates an overall rise in parameters' concentration toward the south, thus degradation of surface water quality in the southerly direction. Given that the Chattahoochee River runs from north to south, this raises an important question as to why Ca, Fe, and pH decrease toward the south (northward rise). The upper Chattahoochee area is important in the sense of providing input to the water that comes into the Atlanta Metro area. Geology, soil, factories, farms, and other areas in the upper Chattahoochee area are variable over time and space as well as the chemistry of water farther north. As a contaminant migrates from sources, concentrations would decrease near the source with time. This can be confirmed with the increasing trends of parameters toward the south as the contaminant diffuses away from the northern sources. Moreover, new contaminant sources showing up toward the north between 2009 to 2019 could be a good reason why Ca, Fe, and pH decrease toward the south (Figures 4.9; 4.8; 4.9). This finding is consistent with a study conducted by He et al., in 2014. The authors modeled the spatial distributions of point and nonpoint source loading potential in the

Saginaw Bay Basin, Michigan, USA. He et al (2014) found that the major part of the total nutrient loading in the watershed is from both point and nonpoint sources. A non-point source has the largest contribution in the nutrient loading among the studied watersheds, especially in the rural watershed.

5.2 Geochemical Processes and Sources of Contamination

Principal Component Analysis (PCA) of water quality variables allows for understanding the source and distribution of sources of contamination as well as principal parameters governing the geochemical process in the study area. The PCA results reveal five significant PCs explaining 84.228 % of the total variance. It is seen from Table 4.7 that the PC I is characterized by strong positive loading of Mg, Na, K, Cl, EC, Mn, moderate positive loading of Ca, Ni, and weak positive loading of SiO2, pH. The PC II is characterized by strong positive loading of SO4, Zn, and moderate positive loading of Ca, Fe, NO3, Ni. PC I and PC II account respectively 41.994% and 15.811% variance in the data. Strong loadings of magnesium, sodium, and potassium from the PC I indicate a contribution of rock minerals weathering, and strong loadings of chloride, EC, and sulfate suggest deposition from dust material and contribution from precipitation (Subba Rao et al., 2006, Machiwal and Jha, 2015). The presence of nitrate in the surface water (positive loading in the PC II) is attributed to anthropogenic sources related to agriculture, nutrient inputs, sewage system, fertilizers, irrigation, etc. The PC III, accounting for 11.419% variance in the data, is characterized by strong positive loading of pH, which Ozler, 2003 attributed to the dissolution of silicate mineral due to reaction with CO_2 (Ozler, 2003).

Furthermore, Table 4.7 reveals multiple strong positive correlations and weak to moderate negative correlations between metals such as Fe, Cu, Cr, Ni, Mn, Pb, and Zn. According to Miller

et al.2014, dissolved metals in waters can have a variety of sources. These include anthropogenic inputs, weathering of parent rock, and rainwater (Miller et al, 2014).

A strong positive correlation between Pb and Cu, and between Fe, Ni, Zn indicate a common origin source and that the metals were transported together during geochemical processes (Bhuiyan et al. 2010). It should also be noted that no strong correlations were found between Cr, Zn, and other dissolved metals in this study. This indicates that a combination of geochemical processes controls Cr and Zn concentrations as well as their mixed associations (Chen et al, 2019). Finally, no significant correlations were found between pH and dissolved metals.

5.3 Correlation of Sources of Contamination with Lineament and LULC

Significant correlations of sources of contamination with high lineament density values were found in this study (Figure 5.1). As contaminants pathways and transport in fractured rock aquifers are mainly controlled by lineaments and their properties, this indicates that the areas with maximum intersection points of the lineaments (high lineament density) are highly susceptible to groundwater contamination from contaminant sources. The lineament data, especially the maximum intersection points of the lineaments, give a sense of fractured rock permeability that conducts surface waters to groundwater. This way, ions in the surface water may contaminate groundwater.

This could be confirmed by comparing data from wells that are located near the intersection points with those in the nearby river stations if groundwater data were available in the study area. However, these findings in the study area are consistent with previous studies, that have revealed a close relationship between lineaments (or lineament density) and groundwater flow and contamination (Sander et al, 1997, Abdulla et al, 2014).

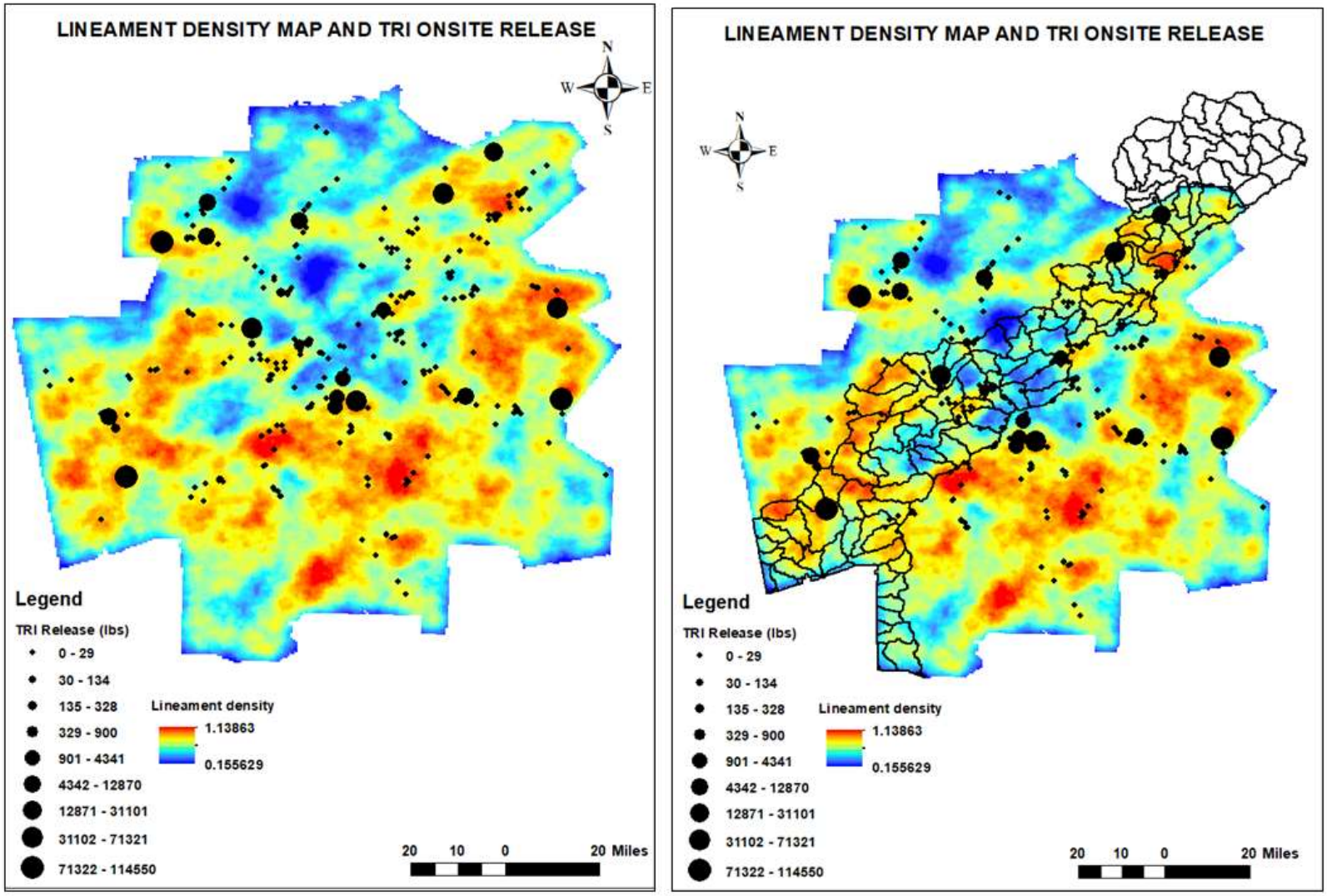

Figure 5-1 Correlations between Lineament Density Map and TRI Onsite Release in 2019

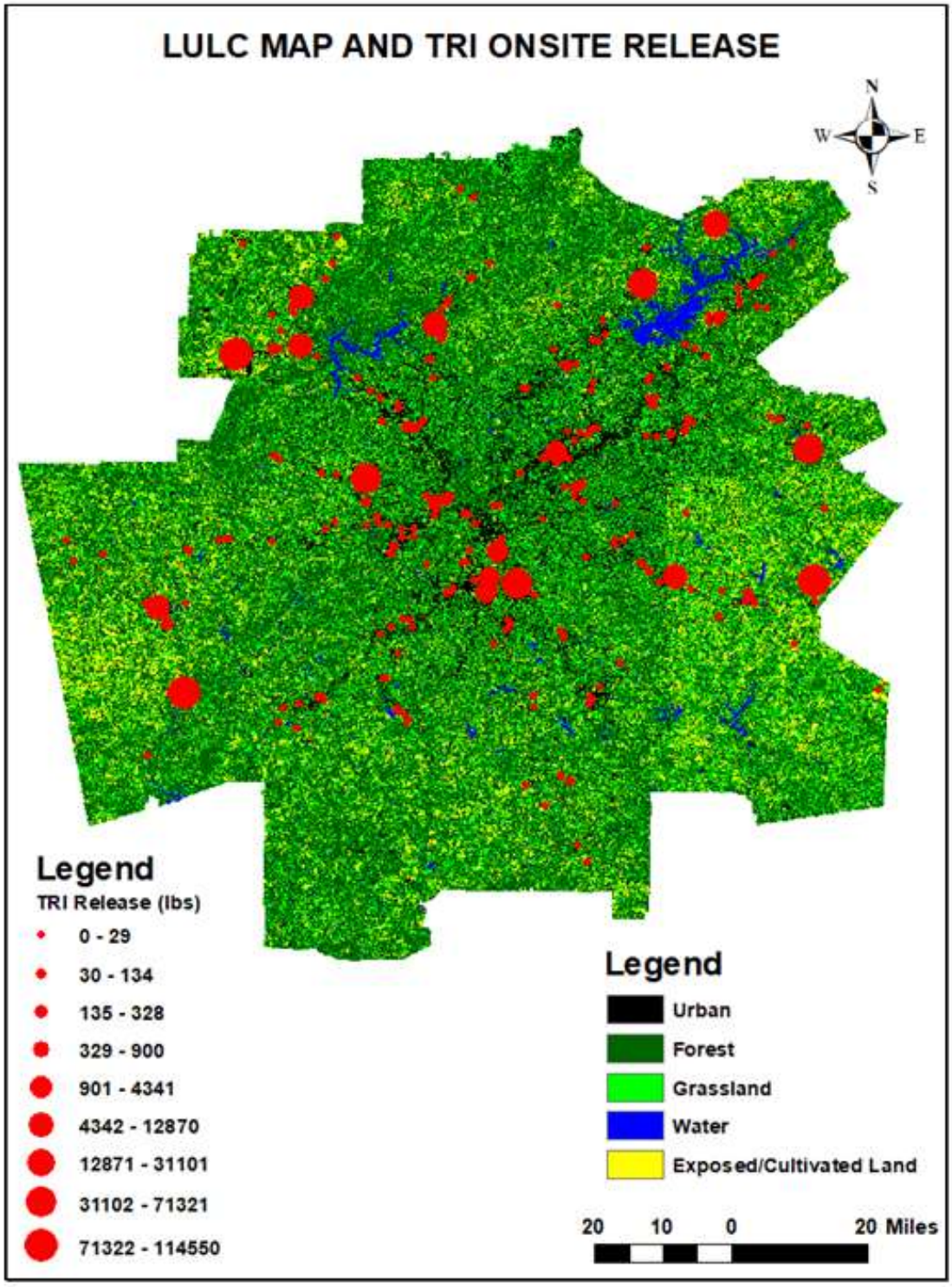

Figure 5-2 Correlations between LULC and TRI Onsite Release in 2019

5.4 Correlation of Sources of Contaminations with Low-Income Communities and People of Color

This study correlated spatial distribution of TRI facilities and the total quantity of chemicals released across the Atlanta metropolitan with income, race, age, and sex using county-level census data to assess the environmental justice in the study area. The results indicate a disproportionate exposure to environmental hazards (TRI facilities and hazardous chemicals.) based on income, race, age, and sex, and therefore no application of environmental justice principles to the area. Low-income and black neighborhoods are more exposed to contaminants (water discharges, landfills, contaminated sites, recycling areas, transfer stations, etc.). This environmental racism includes all kinds of chemicals that cause cancer or other chronic human health effects, significant adverse acute human health effects, and significant adverse environmental effects (TRI Chemical List). The pattern of environmental inequity is more significant in the racial case compared to household income. This finding is in line with Bullard et al study in 2007, which examined toxic wastes and race in the United States. Bullard et al study found race to be more efficient than household income for predicting the location of hazardous waste facilities in the United States.

This shows how polluters have grossly taken advantage of minority and poorer communities, who are disproportionately affected. These people are facing the highest impact, including more asthma, and a high likelihood of heart attacks and premature death.

Furthermore, it is also revealed that central metropolitan counties (Gwinnett, Fulton, Cobb, Cherokee, Forsyth, Paulding, Coweta, Fayette, and Henry) concentrate more TRI facilities in 2019 compared to other counties. These counties are characterized by a high presence of black population or a high ratio of black over white. Also, quite a few southern counties such as Coweta, Fayette, Henry, Newton, Jasper, Lamar, Pike, Meriweather, and Coweta have no chemicals

released and/or record less to no TRI facilities in 2019. However, a high quantity of chemicals was recorded in some northern counties with a high fraction of white population (Bartow, Cherokee, and Hall) along with linear pattern distribution of the TRI facilities in these counties. This high TRI concentration is due to the fact that one of the largest coal-fired power plants in North America called Bowen Steam Electric Generating Plant operates on the northern side of the study area. Bowen Steam Plant (or Plant Bowen) is a coal-fired power station located in Bartow county (outside Euharlee city). It is owned and operated by Georgia Power Company (Southern Company), and is a 2,000-acre coal-fired power plant producing 3,450 megawatts of electricity. Moreover, Cherokee and Hall counties concentrate different types of industries such as electric utilities, machinery, chemical, and metal. For instance, Isotec International Inc and Meyn America LLC operate in Cherokee county producing chemical and polymer products and food products machinery, respectively. Finally, Kubota Manufacturing of America Corp and PPG Archictureal Finishes Inc are among the most important factories operating in Hall county. They respectively manufacture lawn and garden equipment, and paint products (paint, stains, primers, coatings, lacquers, and caulk).

5.5 Limitations

This research has a number of limitations related to data sufficiency and methodology. First of all, this research used two decades of data (2000 to 2019) of 18 surface water parameters (Ca, Mg, Na, K, Fe, SO4, Cl, NO3, SiO2, EC, pH, P, Cu, Cr, Ni, Mn, Pb, Zn). Since only one station was available for parameters Na, K, Fe, SO_4, Cl, Cr, Ni, Mn in 2019, the annual mean values for those parameters were estimated based on the temporal trend and defined pattern of change in the values of the missing parameters. Secondly, the box and whisker plots depicting the variation of the surface water quality parameters for 20 years were performed using a 3-year time lag due to a lack

of yearly data (no consistency of yearly data availability). Thus, yearly variations in the water quality parameters from 2000 to 2019 could not be performed. Furthermore, there has been no Georgia Geologic Survey (GGS) since 2004 and there are no shapefiles of geologic or soil maps of Georgia. In the absence of GGS, only .pdf files are available on the Georgia EPD website. Therefore, the influence of geology and soils on the water contaminations and the correlation of sample sites to geology and soils were not performed in this research. However, the influences of other natural processes such as land use and land cover, and lineaments data (fracture/fault networks) have been analyzed. Finally, county-level data were used in the environmental justice assessment due to the no consistent availability of demographic data at the census tract level in 2019. Thus, the environmental justice assessment may be limited and could be improved by using a fine spatial resolution of demographic data, as counties in the Atlanta metropolitan are not homogenous from north to the south regarding socio-economic status.

5.6 Future Recommendations

Since groundwater quality data are not available in the study area and/or are out of scope in terms of time, future research should install groundwater monitoring wells across the Atlanta metro area around the Chattahoochee River Basin to collect groundwater samples. The collected samples should be analyzed to determine groundwater quality parameters such as Ca, Mg, Na, K, Fe, SO4, Cl, NO3, SiO2, EC, pH, P, Cu, Cr, Ni, Mn, Pb, Zn. All collected data should be checked for regularity without any gaps. Then, these pre-processed data should be used to perform univariate and multivariate statistical analyses, GIS-based geostatistical modeling, and determining the Groundwater Quality Index. The analyses should also include a correlation between surface water, groundwater, lineament data, and sources of contamination.

Furthermore, future research should also assess the intrinsic vulnerability of the study area's aquifer systems to contamination using the DRASTIC model and modified DRASTIC model. The model should take into account the most significant hydrogeologic factors contributing to groundwater contamination in the study area. These include depth to groundwater, net recharge, aquifer media, soil media, topography, impact of the vadose zone, and hydraulic conductivity. A series of ratings and weights should be assigned to these factors depending on the degree of the significance of each parameter that influences the pollution potential. Moreover, the DRASTIC model should be combined with the fracture/fault data (lineament) and land use and land cover to evaluate their influence on the risk of contamination of the aquifer.

Also, regarding the environmental justice assessment, future studies could break down age into different categories (Child, Adolescent, Adult, etc.) and correlate them with the spatial distribution of the TRI to check what category is more exposed to environmental hazards. Further analysis is necessary in the environmental justice analysis to understand demographic data and compare different races in the study area.

Finally, a successful classification of water sampling sites through hierarchical cluster analysis is recommended. The cluster analysis (CA) determines if groundwater sampling sites can be grouped into statistically distinct hydrochemical classes or 'clusters. This classification is correlated to geology to help identify groups of the sites according to sources of contamination.

REFERENCES

Adhikary, P.P., et al., (2015). GIS applicability to assess Spatio-temporal variation of groundwater quality and sustainable use for irrigation. Arabian Journal of Geosciences. 8. 2699-2711. 10.1007/s12517-014-1415-x.

Aller, L., Bennet, T., Lehr, J. H., Petty, R. J., Hackett, G., 1987. "DRASTIC: A Standardized System for Evaluating Ground Water Pollution Potential Using Hydrogeologic Settings." US EPA Report 600/2-87/035, U.S. Environmental Protection Agency.

Bhuiyan, M. A., Parvez, L., Islam, M. A., Dampare, S. B., & Suzuki, S. (2010). Heavy metal pollution of coal mineaffected agricultural soils in the northern part of Bangladesh. Journal of Hazardous Materials, 173(1–3), 384–392.

Bolin, B., Matranga, E., Hackett, E.J., Sadalla, E.K., Pijawka, K.D., Brewer, D., Sicotte, D, (2000). Environmental equity in a sunbelt city: the spatial distribution of toxic hazards in Phoenix, Arizona. Environ Hazards 2:11–24.

Bullard, R.D., et al., (2007). An Open Letter to the Members of Congress: Toxic Wastes and Race at Twenty, 1987-2007: Grassroots Struggles to Dismantle.

Burke, L. M., (1993). Race and Environmental Equity: A Geographic Analysis in Los Angeles, Geo Info Systems, October 1993.

Chakraborty, S., Paul, P.K., Sikdar, P.K., (2007). Assessing aquifer vulnerability to arsenic pollution using DRASTIC and GIS of North Bengal Plain: a case study of English Bazar Block, Malda District, West Bengal, India. J Spat Hydrol 7(1):101–121.

Chen, Y., Wang, L., Liang, T. *et al.* Major ion and dissolved heavy metal geochemistry, distribution, and relationship in the overlying water of Dongting Lake, China. *Environ Geochem Health* **41,** 1091–1104 (2019). https://doi.org/10.1007/s10653-018-0204-y

City of Atlanta (2009). *Pipe Bursting*. http://www.cleanwateratlanta.org/SSES/,Clean Water Atlanta. March 23, 2015.

Cook, J., (2018). Chattahoochee River. https://garivers.org/chattahoochee-river/. Georgia River Network. March 2018.

Cressie, N., Majure, J., (1998). Spatio-Temporal Statistical Modeling of Livestock Waste in Streams. Journal of Agricultural, Biological, and Environmental Statistics: Springer, Vol. 2, No. 1 (Mar. 1997), pp. 24-47.

David, D., (2012). "Environmental Justice on my Mind: Moving Georgia's Environmental Protection Division Toward the Consideration of Environmental Justice in Permitting," *Environmental and Earth Law Journal (EELJ)*: Vol. 2: Iss. 1, Article 3.

Dusen, C., et al., (2017). The complete Guide To The Chattahoochee River .https://www.atlantamagazine.com/.Atlanta Magazine. August 10, 2017.

EPA (1999). US, Georgia, and Atlanta Reach Settlement to Fix City's Aging Sewer System.http://yosemite.epa.gov/. July 29, 1999.

EPA (2012). What is Nonpoint Source Pollution? http://water.epa.gov/polwaste/nps/whatis.cfm, U.S. Environmental Protection Agency, March 6, 2012.

EPA (2018). Ensuring clean and safe water. U.S. Environmental Protection Agency Office of Inspector General. Report No. 18-P-0206.May 30, 2018.

Forina, M., et al., (2005). Methods of Varimax rotation in factor analysis with applications in clinical and food chemistry, Journal of Chemometrics 3(S1):115-125. DOI:10.1002/cem.1180030504

He, C., et al., (2014). Estimating point and non-point source nutrient loads in the Saginaw Bay watersheds, Journal of Great Lakes Watersheds, Volume 40, Supplement 1, 2014, Pages 11-17. February 11, 2014.

Jabbar, F.K., Grote, K., (2019). Statistical assessment of nonpoint source pollution in agricultural watersheds in the Lower Grand River watershed, MO, USA. Environ Sci Pollut Res 26, 1487–1506 (2019). https://doi.org/10.1007/s11356-018-3682-7.

Khabo-Mmekoa, C. M. N., Momba M. N. B., (2019). The Impact of Social Disparities on Microbiological Quality of Drinking Water Supply in Ugu District Municipality of Kwazulu-Natal Province, South Africa, Int J Environ Res Public Health. 2019 Aug; 16(16): 2972. DOI: 10.3390/ijerph16162972.

MacDonald, G.J., Defelice, N., Sebastian, D., Leker, H., (2014). Racial disparities in access to community water supply service in Wake County, North Carolina. Front. Public Health Serv. Syst. Res. **2014**, 3, 25–35.

Machiwal, D., Jha, M.K., (2010). Tools and techniques for water quality interpretation. In: Krantzberg, G., Tanik, A., Antunes do Carmo, J.S., Indarto, A., Ekdal, A. (Eds.), Advances in Water Quality Control. Scientific Research Publishing, Inc., California, USA, pp. 211–252.

Machiwal, D., Jha, M., (2015). Identifying sources of groundwater contamination in a hard-rock aquifer system using multivariate statistical analyses and GIS-based geostatistical modeling techniques. Journal of Hydrology: Regional Studies. 13. 10.1016/j.ejrh.2014.11.005.

Miller, H., Croudace, I. W., Bull, J. M., Cotterill, C. J., Dix, J.K., & Taylor, R. N. (2014). A 500-year sediment lake record of anthropogenic and natural inputs to Windermere (English Lake District) using double-spike lead isotopes, radiochronology, and sediment microanalysis. Environmental Science and Technology, 48(13), 7254–7263.

Ozler, H.M., 2003. Hydrochemistry and salt-water intrusion in the Van aquifer, east Turkey. Environ. Geol. 43, 759–775. Rivest, M., Marcotte, D., Pasquier, P., 2012. Sparse data integration for the interpolation of concentration measurements using kriging in natural coordinates. J. Hydrol. 416–417, 72–82.

Park, Y. M., and Kwan, M-P., 2017. Multi-contextual segregation and environmental justice research: toward fine-scale spatiotemporal approaches. Int. J. Environ. Res. Public Health, 14(10), 1205; https://doi.org/10.3390/ijerph14101205.

Pasetto, R., Mattioli, B., Marsili, D., (2019). Environmental Justice in Industrially Contaminated Sites. A Review of Scientific Evidence in the WHO European Region. *International Journal of Environmental Research and Public Health.*19 March 2019.

Rose, S., Peter, N.E., (2001). Effects of urbanization on streamflow in the Atlanta area (Georgia, USA): a comparative hydrological approach: Hydrological Processes 15, p. 1,441–1,457.

Sander P, Minor TB, Chesley MM. Groundwater exploration based on lineament analysis and reproducibility tests. Ground Water 1997; 35(5): 888-94.

Satterthwaite, D., Mcgranahan G., Tacoli C., (2010). Urbanization and its implications for food and farming. Philos Trans R Soc Lond B Biol Sci. 2010 Sep 27; 365(1554): 2809–2820. DOI: 10.1098/rstb.2010.0136.

Schaider, L.A., Swetschinski, L., Campbell, C., and Rudel, R. A., 2019. Environmental justice and drinking water quality: are there socioeconomic disparities in nitrate levels in U.S. drinking water? Environ Health 18, 3 (2019). https://doi.org/10.1186/s12940-018-0442-6.

Shabnam, N., Sharmila, P., Pardha-Saradhi, P., (2017). Impact of ionic and nanoparticle speciation states of silver on light harnessing photosynthetic events in Spirodela polyrhiza. Int. J. Phytoremediat. 19, 80–86. DOI: 10.1080/ 15226514.2016.1216083.

Shirazi, S., Imran, H., Akib, S., (2012). GIS-based DRASTIC method for groundwater vulnerability assessment: A review. Journal of Risk Research 15(8), 2012, 991-1011.

Shirazi, S.M., Imran, H.M., Akib, S., Yusop, Z., Harun, Z.B., (2013). Groundwater vulnerability assessment in the Melaka State of Malaysia using DRASTIC and GIS techniques. Environ Earth Sci 70:2293–2304.

Stack & Associates (2018). Dedicated to the Environment. https://www.stackenvirolaw.com/.Monday, April 9, 2018.

Subba Rao, N., John Devadas, D., Srinivasa Rao, K.V., 2006. Interpretation of groundwater quality using principal component analysis from Anantapur district, Andhra Pradesh, India. Environ. Geosci. 13 (4), 239–259.

Tu, J., (2011). Spatial and temporal relationships between water quality and land use in northern Georgia, USA, Journal of Integrative Environmental Sciences, 8:3, 151-170, DOI: 10.1080/1943815X.2011.577076.

Yang, X., Lo, C. P., (2003). Modeling Urban Growth and Landscape Change for the Atlanta Metropolitan Region. International Journal of Geographical Information Science, 17, 463-488.

Zimmerman, R., (1993). Social Equity and Environmental Risk, Risk Analysis, 13, 649-666.